

**NASA CONTRACTOR  
REPORT**

**NASA CR-170**



**NASA-TCR**

0099804



**A THEORY FOR THE OPTIMAL  
DETERMINISTIC CHARACTERIZATION  
OF THE TIME-VARYING DYNAMICS  
OF THE HUMAN OPERATOR**

*by Walter W. Wierwille and Gilbert A. Gagne*

Prepared under Contract No. NAS 1-3485 by  
CORNELL AERONAUTICAL LABORATORY, INC.  
Buffalo, N. Y.  
*for*

NATIONAL AERONAUTICS AND SPACE ADMINISTRATION • WASHINGTON, D. C. • FEBRUARY 1965



A THEORY FOR THE OPTIMAL DETERMINISTIC CHARACTERIZATION  
OF THE TIME-VARYING DYNAMICS OF THE HUMAN OPERATOR

By Walter W. Wierwille and Gilbert A. Gagne

Distribution of this report is provided in the interest of  
information exchange. Responsibility for the contents  
resides in the author or organization that prepared it.

Prepared under Contract No. NAS 1-3485  
CORNELL AERONAUTICAL LABORATORY, INC.  
Buffalo, N. Y.

for

NATIONAL AERONAUTICS AND SPACE ADMINISTRATION

---

For sale by the Office of Technical Services, Department of Commerce,  
Washington, D.C. 20230 -- Price \$3.00

# A THEORY FOR THE OPTIMAL DETERMINISTIC CHARACTERIZATION OF THE TIME-VARYING DYNAMICS OF THE HUMAN OPERATOR

By Walter W. Wierwille and Gilbert A. Gagne

Cornell Aeronautical Laboratory, Inc.  
of Cornell University

## SUMMARY

A deterministic theory of characterization is presented which can be used to determine the time-varying dynamics of the human operator engaged in a tracking task. With this theory it is possible to obtain a time-varying impulse response and a time-varying transfer function which represent the action of a human operator in an open- or closed-loop control system. No special form of input is required.

The characterization, which may be developed for either real-time or non-real-time computation, is based upon an exact theory of fixed-form optimization. A strongly convergent, definitely stable, iteration technique can be used to realize the optimal characterization filter. The theory takes the time-variation of the impulse response or transfer function into account, so that it is unnecessary to make the assumption of slowly varying dynamics.

An uncertainty or compromise is shown to exist between the error (that is, the error between the output of the human operator and that of the optimal characterizing filter) and the degree of time-variability of the optimal characterizing filter. This uncertainty appears to be fundamental, and cannot be circumvented.

A number of experiments which verify and make use of the theory are presented. Known time-varying networks can be accurately characterized, and changes in the tracking transfer characteristic of the human operator can be detected.

## INTRODUCTION

Two general approaches have been used in the past for the characterization of the time-varying dynamics of human operators engaged in tracking tasks. The first approach is statistical in nature and involves the estimation of parameters within specified confidence limits by finite time averages of data.<sup>1</sup> From this information, it is possible to obtain a slowly time-varying characterization model. The second approach is deterministic in nature and involves the convergence of error by varying model parameters according to the method of steepest descent.<sup>2,3</sup> In this case the parameters can be permitted to vary rapidly; but since the dynamics are changing, the underlying theory is only approximate. Other techniques have also been used for determining time-varying human operator dynamics, but they require restricted classes of input signals.<sup>4</sup>

This report presents an alternative theory of time-varying characterization, which is also deterministic. It differs from other deterministic approaches by the way in which the time variation is taken into account. In the sense of the chosen performance measure, this time-varying characterization scheme is optimum, and no approximations are required in theory.

This new approach incorporates a performance measure which permits minimization of error between the human operator's output signal and that of a mathematical model. However, the minimization is subjected to a constraint on the change allowed in each time-varying parameter in the model. The constraint itself contains an arbitrary constant which determines the relative emphasis to be placed on parameter variation as compared with tolerated error. This compromise (or trade-off) between parameter variation and modeling error is fundamental to the deterministic time-varying characterization problem.

The approach which is to be presented makes use of a model filter of fixed form. This filter is composed of a group of fixed component filters whose inputs are connected to the display input signal,\* and whose output gains are to be varied as functions of time and then summed. The characterization procedure to be described is not limited to the use of linear filters, since the component filters may be nonlinear if desired.

---

\*If a compensatory display is used, the single input (or error) signal to the display is also impressed upon the inputs to the model component filters. If a pursuit display is used, the input to the model filters should be obtained by subtracting the system output signal from the system input signal, thereby artificially obtaining an error signal.

The problem with which this report deals and which this new characterization approach is capable of solving is the following:

- Given:           The input signal (an analog form of which is displayed to the operator) and corresponding output signal (proportional to control stick deflection) of a human operator for a specified time interval.
- Determine:       The time-varying transfer characteristic\* from a specified class which most accurately characterizes (subject to a required constraint) the human operator during the given time interval.

It is important to realize that the solution of this problem for a particular case is not generally amenable to extrapolation or generalization. If the input signal is changed, if the control system configuration is changed, or even if the problem is rerun in real time with the same human operator, one cannot expect to obtain exactly the same results. On the other hand, this approach does answer the question, "What was the human operator's time-varying transfer characteristic for a particular tracking task?" As such, the approach is meaningful, for it allows quantitative evaluations of specific control situations. It is particularly well suited for detecting changes in the human operator's transfer characteristic.

If it is assumed for the moment that deterministic time-varying transfer characteristics are obtainable, there remains the question of how to use these characteristics so as to yield valid extrapolative results. The answer involves a straightforward application of mathematical statistics. Experimental situations often arise in which deterministic data have been collected for a number of subjects under controlled experimental conditions. The objective is to draw valid generalizations by performing statistical tests which make use of the data from all the subjects. An example is that of gathering tracking error data for a number of subjects to compare two different tracking displays. If a sufficient number of subjects are tested, and if the experiment is properly controlled, it is possible to determine which display is better, using some measure of error as a criterion. In a similar manner, the deterministic time-varying transfer characteristics of a number of subjects can be obtained under controlled experimental conditions. These data can then be statistically analyzed so that valid extrapolative results are obtained. Those factors which may cause changes in the human operator's response over time can be carefully and accurately studied using this method. The effects of fatigue, learning, changes in input signal, changes in controlled dynamics, and changes in environment on the human operator's transfer characteristic can be studied and generalized. This approach to time-varying characterization will permit valid extrapolative results.

---

\* A transfer characteristic is any mathematical function which is used to describe the relationship between the input and output signals of the human operator. It may be an impulse response function, or a transfer function, or another type of mathematical description.

## Acknowledgments

The work described herein was supported in its entirety by the National Aeronautics and Space Administration, Langley Research Center, Hampton, Virginia, under Contract NAS 1-3485. The contract technical monitor was Mr. James J. Adams, of the Guidance and Control Branch. The authors wish to express their thanks to Mr. Adams and his colleagues for their helpful participation in this project, particularly in data-collection.

Thanks also go to Dr. William C. Schultz of Cornell Aeronautical Laboratory for many helpful suggestions throughout the course of this investigation. Lastly, the authors wish to thank Mr. James Knight for his highly versatile technical help.

## BACKGROUND

The deterministic characterization theory affords a method whereby the time-varying dynamics of the human operator may be characterized.

If this theory is to be described in a logical manner, it is necessary that a certain amount of background information be given beforehand.

This information hopefully makes it possible to avoid the misunderstanding of terms which have been defined in differing ways in the technical literature and provides an appropriate setting for the time-varying characterization problem.

### Network Theory For Characterization

A very important aspect of time-varying characterization of the human operator is the development of a suitable time-variable network theory. It would be desirable for such a theory to possess the following properties:

- (1) It must be capable of mathematically specifying the relationship between the input signal and the output signal of any linear, time-varying network.
- (2) It should allow the development of concepts such as time-varying impulse response and time-varying transfer function, both of which degenerate to the usual definitions for the fixed (non-time-varying) case.
- (3) It should allow as an extension the capability for describing special classes of nonlinear time-varying networks.

- (4) It must mathematically describe a broad class of linear time-varying characterization network models which are known to represent the human operator, and
- (5) The network theory and chosen class of models must allow the development of a deterministic theory of characterization.

It is possible to develop a network theory which possesses all of the above properties.\*

Let the impulse response,  $h(t, \tau)$ , of a time-varying linear network be defined as the response at time  $t$  to a unit impulse applied  $\tau$  seconds earlier than  $t$ .\*\* If  $h(t, \tau)$  is realizable, then  $h(t, \tau) = 0$  for  $\tau < 0$ . Then, since any realizable input signal,  $x(t)$ , can be considered to be composed of a group of weighted impulses,<sup>5</sup> the output  $z(t)$  is given by an extended form of the convolution integral:

$$z(t) = \int_{-\infty}^{\infty} h(t, \tau) x(t - \tau) d\tau = \int_{-\infty}^{\infty} x(\lambda) h(t, t - \lambda) d\lambda \quad (1)$$

This form of the convolution integral is an exact description of the relation between the input and output of a time-variable network. It reduces to the usual (constant-coefficient) case for  $h(t, \tau) = h(0, \tau)$ ; that is, if the impulse response is non-time varying.

The transfer function (or frequency response) of a time-varying linear network is defined as the Fourier transform of the impulse response with  $t$  treated as a constant under the integral. Thus,

$$H(t, j\omega) = \int_{-\infty}^{\infty} h(t, \tau) e^{-j\omega\tau} d\tau \quad (2)$$

The inverse theorem relating the time-varying transfer function to the time-varying impulse response can be derived without difficulty, yielding

$$h(t, \tau) = \frac{1}{2\pi} \int_{-\infty}^{\infty} H(t, j\omega) e^{j\omega\tau} d\omega \quad (3)$$

These definitions for the impulse response and frequency response are similar to those of Zadeh.<sup>6</sup> They have been chosen because they allow the

---

\* Most of the theory has been previously presented in the literature. However, the method of presentation is original.

\*\* Mathematical symbols are defined as they are introduced in the text. Appendix A also lists and defines each symbol.

development of a theory possessing the five properties discussed earlier.

A number of important theorems for time-variable networks can be proved by the use of the above definitions. Among them are the following:

$$z(t) = \frac{1}{2\pi} \int_{-\infty}^{\infty} H(t, j\omega) X(j\omega) e^{j\omega t} d\omega \quad (4)$$

and

$$Z(ju) = \frac{1}{2\pi} \int_{-\infty}^{\infty} X(j\omega) \kappa(ju - j\omega, j\omega) d\omega \quad (5)$$

where  $X(j\omega)$  is the Fourier transform of  $x(t)$   
 $Z(j\omega)$  is the Fourier transform of  $z(t)$ ,

and 
$$\kappa(ju, j\omega) = \int_{-\infty}^{\infty} H(t, j\omega) e^{-jut} dt \quad (6)$$

The theorem given by equation (4) states that the time response of a time-variable network is obtained by taking the inverse Fourier transform of the product of the time-varying transfer function and the Fourier transform of the input signal. The theorem of equation (5) is the frequency domain dual of equation (1).<sup>7</sup>

The previously described set of definitions and theorems constitutes an elementary, but very general, approach to time-variable network theory which can be used for the characterization problem. With this theory, it is possible to describe the relationship between the input and output of any linear time-varying network. Because of this generality, the mathematical derivations for an optimal deterministic theory would be too complicated to be of value in practice. In particular, time-varying integral equations would have to be solved for this general case. It is better to limit the class of admissible filtering operations at the outset, so that exact practical solutions are obtained for the class. If one views all linear time-varying filters as a certain class, one realizes that the choice of a class is arbitrary. Therefore, it is reasonable to choose that class of filters which is sufficiently general for accurate characterization, but which also allows straightforward solution for the optimal filter within the class.

Let it be assumed that a network configuration such as that shown in Fig. 1 is to be used for characterization. This configuration is described by a set of previously specified linear constant-coefficient networks called component filters, followed by a group of time-varying gains. For the  $i^{th}$  filter, the impulse response is given by  $h_i(\tau)$  and the transfer function is given by  $H_i(j\omega)$ . The weighted outputs are summed to produce the model output,  $z(t)$ . The output of this network configuration may be expressed as



$$z(t) = \sum_{i=1}^K a_i(t) x_i(t) \quad (7)$$

$$= \sum_{i=1}^K a_i(t) \int_{-\infty}^{\infty} h_i(\tau) x(t-\tau) d\tau \quad (8)$$

$$= \int_{-\infty}^{\infty} \left[ \sum_{i=1}^K a_i(t) h_i(\tau) \right] x(t-\tau) d\tau \quad (9)$$

Upon comparison of equation (9) with equation (1) it is seen that the series may be represented by

$$h(t, \tau) = \sum_{i=1}^K a_i(t) h_i(\tau) \quad (10)$$

Therefore, this network configuration represents a subclass of the class of all time-varying linear networks. It has the great advantage of allowing direct computation of the time-varying impulse response from the time-varying gains. Since the impulse response of each component filter is fixed, it is only necessary for any given instant of time,  $t$ , to weight these impulse responses with the gains,  $a_i(t)$ , and add the results. Thus, the model or network configuration is directly translatable into the time-varying impulse response description.

This property of direct translation to impulse response is not generally valid for networks other than those that can be drawn in a configuration like that of Fig. 1. To illustrate this fact, assume for example that the time-varying gains were placed ahead of the fixed component filters. In this case the response,  $z(t)$ , is given by

$$z(t) = \sum_{i=1}^K \int_{-\infty}^{\infty} h_i(\tau) x(t-\tau) a_i(t-\tau) d\tau \quad (11)$$

Clearly, the time-varying gains cannot be removed from the integrals. The time-varying impulse response therefore cannot be written as a sum of separable products; that is, in general,

$$h(t, \tau) \neq \sum_{i=1}^K b_i(t) g_i(\tau) \quad (12)$$

where  $b_i(t)$  and  $g_i(\tau)$  are arbitrary functions each of a single independent variable.

The model of Fig. 1 also allows the straightforward determination of the time-varying transfer function. Consider that equation (8) may be rewritten such that

$$z(t) = \sum_{i=1}^K a_i(t) \frac{1}{2\pi} \int_{-\infty}^{\infty} H_i(j\omega) X(j\omega) e^{j\omega t} d\omega \quad (13)$$

$$= \frac{1}{2\pi} \int_{-\infty}^{\infty} \left[ \sum_{i=1}^K a_i(t) H_i(j\omega) \right] X(j\omega) e^{j\omega t} d\omega \quad (14)$$

Upon comparison of equation (14) with equation (4), it is seen that the series may be represented by

$$H(t, j\omega) = \sum_{i=1}^K a_i(t) H_i(j\omega) \quad (15)$$

Once again, the separability property is valid for this subclass. The time-varying transfer function can therefore be obtained at any time,  $t$ , by weighting the fixed transfer functions,  $H_i(j\omega)$ , with their corresponding gains,  $a_i(t)$ , and summing the results.

It has been shown that the modeling configuration of Fig. 1 allows the straightforward determination of the time-varying impulse response or time-varying transfer function. Therefore, there is no problem, in theory, in translating this model into usable mathematical quantities.

The question now arises as to whether the model configuration chosen is restrictive in the sense that it represents a sufficiently broad class of filters for characterizing the human operator. The results of other investigators indicate that, if the fixed component filters are properly chosen, relatively high accuracy is obtainable in characterizing systems.<sup>8, 9</sup> In addition, human operator characterization may be accomplished with five or six component filters if they are properly chosen.<sup>1</sup> It may be concluded from previous work that the choice of the modeling configuration of Fig. 1 is not significantly restrictive. The choice of the filters will be discussed in greater detail in the section on experimental verification.

The concepts described above for linear filters can be extended in a logical manner to cover nonlinear networks. However, in the nonlinear case, Fourier (frequency domain) representations appear to be of little practical value, so that time domain representations only will be used. In dealing with nonlinear networks, general classes must be specified within which the admissible networks must be described. One widely used set of classes is the set of  $N_n$  classes.<sup>10</sup> The response of a class  $N_n$  network to an input  $x(t)$  is given by

$$z(t) = \int_0^\infty \int_0^\infty \dots \int_0^\infty J[x(t-\tau_1), x(t-\tau_2), \dots, x(t-\tau_n), \tau_1, \tau_2, \dots, \tau_n, t] d\tau_1 d\tau_2 \dots d\tau_n \quad (16)$$

where  $J[x(t-\tau_1), x(t-\tau_2), \dots, x(t-\tau_n), \tau_1, \tau_2, \dots, \tau_n, t]$  is the so-called time-varying kernel function. As  $n$  increases, the class of networks becomes more general. Moreover, the class,  $N_n$ , of networks includes all lower classes, that is,  $N_{n-1}, N_{n-2}, \dots, N_1$ .

If the configuration of Fig. 1 is used, the solution for the optimal coefficients is no more difficult if the fixed component networks are nonlinear than if they are linear. As a consequence, the previous results can be easily extended. Suppose that the specified linear component filters are replaced by nonlinear filters described by

$$x_i(t) = \int_0^\infty \int_0^\infty \dots \int_0^\infty J_i[x(t-\tau_1), x(t-\tau_2), \dots, x(t-\tau_n), \tau_1, \tau_2, \dots, \tau_n] d\tau_1 d\tau_2 \dots d\tau_n \quad (17)$$

Each output  $x_i(t)$  is then the result of a specified, constant coefficient class  $N_n$  nonlinear filtering operation. Upon comparison of equation (16) with equations (7) and (17), it is seen that

$$\begin{aligned} & J[x(t-\tau_1), x(t-\tau_2), \dots, x(t-\tau_n), \tau_1, \tau_2, \dots, \tau_n, t] \\ &= \sum_{i=1}^K a_i(t) J_i[x(t-\tau_1), x(t-\tau_2), \dots, x(t-\tau_n), \tau_1, \tau_2, \dots, \tau_n] \end{aligned} \quad (18)$$

Thus, a subclass of the class,  $N_n$ , of filters has been chosen for characterization.

The major problem which exists when dealing with nonlinear networks for characterization is the difficulty of specifying these networks in relatively simple form. It is clear that the kernel function,  $J$ , is a function with  $2n+1$  independent variables. As a result of this higher dimensionality, translation of a known characterization model into a mathematical function is usually a difficult task. However, in those cases where a modeling description only is required, the nonlinear approach can be readily applied.

### Uncertainty

It is necessary to recognize the basic problem of uncertainty before attempting to understand the theory of deterministic characterization. It has been known for many years that basic uncertainties exist in the simultaneous measurement of certain pairs of quantities. The first uncertainty was discovered in atomic physics.<sup>11</sup> It was shown that there is a lower bound to the

accuracy with which the position and momentum of an electron may be simultaneously determined. The more accurately the position of an electron is determined, the less accurately the momentum can be determined, and vice versa. Uncertainties also exist in communication theory. An example is the fact that the product of the bandwidths of a Fourier transform pair is always greater than or equal to a fundamental constant.<sup>12</sup> Another uncertainty in communication theory exists in the detection of a properly defined non-stationary power spectral density of a signal.<sup>13</sup> The assertion is now made that there is also an uncertainty in the characterization of the time-varying dynamics of the human operator. This uncertainty is fundamental and cannot be circumvented. It is not particularly detrimental to the characterization problem, but it does require that, in addition to the performance measure chosen, an arbitrary constant must also be chosen which resolves the compromise between the error in characterization and the rate at which the transfer characteristic is allowed to change with time. Thus, the theory will permit the error to be made as small as desired, but then the time variation of the transfer characteristic may be excessive. In all cases, a compromise must be reached between error in characterization and allowed time variation of the transfer characteristic.

In the development of the theory emphasis will be placed upon a practical derivation which accounts for this uncertainty. The technique by which a solution is obtained is that of constraining the degree of variability of the time-varying gains of the characterization model. No attempt will be made to rigorously prove the existence of an uncertainty; however, in the steps which must be followed to arrive at a practical solution to the deterministic characterization problem, it will become evident that an uncertainty does exist.

## DETERMINISTIC CHARACTERIZATION THEORY

The central problem of the theory of deterministic characterization is that of the optimal adjustment of the chosen mathematical model so as to minimize the error between the output of the model and that of the human operator. Both the input signal record and the output signal record are assumed to be available over a given time interval for which the characterization is desired.\* The problem of particular interest herein is that of developing a time-varying characterization. Therefore, in the modeling configuration of Fig. 1, the gains following the fixed component filters must be allowed to vary with time, and it is this set of time-varying gains which must be obtained.

It is necessary initially to show that if the time-varying gains are unconstrained, the solution for minimum error is trivial. The trivial solution results from the uncertainty principle.

---

\*The theory will be developed for the non-real-time solution and then will be modified for the real-time solution. A non-real-time solution is one in which the characterization may be obtained after the data for the entire length of the tracking task have been gathered. A real-time solution is one in which the characterization must be obtained while the tracking task is in progress.

Let

$$e(t) = \left[ y(t) - \sum_{i=1}^K a_i(t) x_i(t) \right] \quad (19)$$

where

$e(t)$  is the error in characterization as a function of time,

$y(t)$  is the output of the human operator (the desired output of the model), and

$x_i(t)$  is the response of the  $i^{\text{th}}$  fixed component filter to the input signal  $x(t)$  which the human operator is tracking.

A performance measure which allows minimization of the error while simultaneously allowing analytical solution of the problem is the integral of the squared error over the interval for which data is taken. Therefore, let

$$\theta = \int_0^T e^2(t) dt \quad (20)$$

where  $\theta$  is the performance measure to be minimized,

$t=0$  is the initial point, and

$t=T$  is the final point in the time interval over which a solution is desired.

This problem is of the form

$$\theta = \int_0^T f[t, a_1(t), a_2(t), \dots, a_K(t)] dt \quad (21)$$

where  $f$  is given by squaring both sides of equation (19). The critical values\* of this equation are given by the set of equations

$$\frac{\partial f}{\partial a_l} = 0; \quad l = 1, 2, \dots, K \quad (22)$$

Upon evaluation of this set of equations, one obtains

$$x_l(t) \left[ y(t) - \sum_{i=1}^K a_i(t) x_i(t) \right] = 0 \quad l = 1, 2, \dots, K \quad (23)$$

This condition is satisfied if

$$y(t) = \sum_{i=1}^K a_i(t) x_i(t) \quad \text{when } x_l(t) \neq 0 \quad (24)$$

\*A critical value is defined to be a maximum, a minimum, or an inflection point.

It is also satisfied for any value of  $\alpha_\ell(t)$  if  $x_\ell(t) = 0$ . The optimal conditions indicate that the weighted outputs must equal  $y(t)$ . Thus, instead of having the time-varying gains follow the changes in the human operator's dynamics, the gains simply track the signal itself. Moreover, if at time  $t$  there are  $q$  component filters with nonzero outputs, then there are  $(q-1)$  infinities of possible solutions all giving the same value of minimum error. Thus, the solution is not unique. It can be concluded that, as a result of rapid gain variations and the infinities of possible solutions, that this characterization technique is trivial.

At the opposite extreme of this basic uncertainty is the case in which the time-varying gains have been constrained so severely that they become constants within the characterization interval. This is the case in which all information about the time variation of the dynamics is sacrificed. Let

$$e(t) = \left[ y(t) - \sum_{i=1}^K a_i x_i(t) \right] \quad (25)$$

where each  $a_i$  is a constant. Then, if the same performance measure is minimized, the following condition for the optimal gains must be met:

$$\theta_\ell = \sum_{i=1}^K a_i \theta_{i\ell}; \quad \ell = 1, 2, \dots, K \quad (26)$$

where

$$\theta_\ell = \int_0^T y(t) x_\ell(t) dt \quad (27)$$

$$\theta_{i\ell} = \int_0^T x_i(t) x_\ell(t) dt \quad (28)$$

This is a meaningful solution, but a degenerate one for the time-varying case, since no information about the time variation is obtained. It represents the second extreme case of the uncertainty.

The above two extreme problems suggest that a more useful solution to the time-varying characterization problem can be obtained if the gain changes are constrained, but not so heavily as to be constant. This type of problem can be cast in the form of a calculus-of-variations problem by including the squared values of the rate-of-change of parameters in the performance measure. For example, one might choose the performance measure,

$$\theta = \int_0^T \left[ e^2(t) + \lambda^2 \sum_{i=1}^K \dot{a}_i^2(t) \right] dt \quad (29)$$

where  $\lambda^2$  is the positive constant which determines the relative weight to be placed upon error, as compared with rate of parameter-variation. Since, in

general, both the error and the rate-of-change of all parameters cannot be made zero over the time interval  $0 \leq t \leq T$ , the best compromise (for a given choice of  $\lambda^2$ ) is given by an extremal of the calculus-of-variations solution to this problem.

Unfortunately, the calculus of variations (when applied to this problem) yields a solution which, although meaningful, is very difficult to use. Briefly, the solution is given by a set of simultaneous Euler equations<sup>14</sup>

$$\frac{\partial f}{\partial a_\ell} - \frac{d}{dt} \left( \frac{\partial f}{\partial \dot{a}_\ell} \right) = 0; \quad \ell = 1, 2, \dots, K \quad (30)$$

under the assumptions that

either  $a_\ell(0)$  is specified or  $\dot{a}_\ell(0) = 0$

and that  $a_\ell(T)$  is specified or  $\dot{a}_\ell(T) = 0$

Upon evaluating the Euler equations, a set of simultaneous, unstable second-order, time-varying differential equations results:

$$\ddot{a}_\ell(t) = -\frac{1}{\lambda^2} \left[ y(t) - \sum_{i=1}^K a_i(t) x_i(t) \right] x_\ell(t); \quad \ell = 1, 2, \dots, K \quad (31)$$

which can be rearranged such that

$$\ddot{a}_\ell(t) - \left[ \frac{1}{\lambda^2} x_\ell^2(t) \right] a_\ell(t) = -\frac{1}{\lambda^2} \left[ y(t) - \sum_{\substack{i=1 \\ i \neq \ell}}^K a_i(t) x_i(t) \right] x_\ell(t); \quad \ell = 1, 2, \dots, K \quad (32)$$

No general first integral exists for this set of equations, since the functions  $y(t)$  and all  $x_i(t)$  cannot be generally written in analytical forms. As a consequence, the above set of simultaneous, unstable, two-point boundary value differential equations must be solved directly. It is believed that this type of solution is too difficult to be of practical value, even though the performance measure properly constrains the parameter variation for the time-varying characterization problem.

The problem of the deterministic theory can now be considered to consist of modifying the constraint on the parameter variation so as to allow a more practical solution for the time-varying gains. It is possible to solve the problem of the deterministic theory in another way such that the solutions obtained are not compromised. Moreover, with the use of this new constraint, the time-varying gains are easily computed after a set of simultaneous linear algebraic equations is solved. Consequently, the approach is well-suited to practice.

The method to be used is a so-called "fixed form" method in which a straightforward solution can always be obtained.<sup>15</sup> Let the performance measure of equation (20) again be used. This measure is to be minimized, but the time-varying gains are to be subjected to the fixed form constraint given by

$$a_l(t) \equiv \sum_{m=0}^L \alpha_{ml} \beta_{ml}(t) \quad (33)$$

where each  $\beta_{ml}$  is a known, fixed function of time, and each  $\alpha_{ml}$  is a constant which is to be determined such that the performance measure is minimized. Thus, the problem is constrained by forcing each time-varying gain to be a linear combination of a set of known time functions. Usually, the same set of time functions may be used for each time-varying gain, so that the constraint may be written in a simpler form without serious limitation:

$$a_l(t) = \sum_{m=0}^L \alpha_{ml} \beta_m(t) \quad (34)$$

Of course, the effect of this constraint on the solution for the optimal set of gains is heavily dependent upon the choice of the  $\beta_m(t)$ 's. This point requires extensive discussion and will be considered after the minimization process has been described.

If equations (34) and (19) are substituted into equation (20), the performance measure after manipulation can be written as

$$\begin{aligned} \theta = & \int_0^T y^2(t) dt - 2 \sum_{i=1}^K \sum_{m=0}^L \alpha_{mi} \int_0^T \beta_m(t) x_i(t) y(t) dt \\ & + \sum_{i=1}^K \sum_{m=0}^L \sum_{j=1}^K \sum_{n=0}^L \alpha_{mi} \alpha_{nj} \int_0^T \beta_m(t) \beta_n(t) x_i(t) x_j(t) dt \end{aligned} \quad (35)$$

In order to simplify the notation, let

$$\phi_{mi} \equiv \int_0^T \beta_m(t) x_i(t) y(t) dt \quad (36)$$

and

$$\phi_{minj} \equiv \int_0^T \beta_m(t) \beta_n(t) x_i(t) x_j(t) dt \quad (37)$$

Substitution of equations (36) and (37) into equation (35) yields the fundamental equation which is to be minimized:



$$\theta = \int_0^T y^2(t) dt - 2 \sum_{i=1}^K \sum_{m=0}^L \alpha_{mi} \phi_{mi} + \sum_{i=1}^K \sum_{m=0}^L \sum_{j=1}^K \sum_{n=0}^L \alpha_{mi} \alpha_{nj} \phi_{minj} \quad (38)$$

The minimization will yield the optimal set of  $\alpha_{mi}$ 's which will then allow the computation of the time-varying gains,  $a_i(t)$ . \* Thereafter, the time-varying transfer characteristic can be computed.

The minimization procedure can be more easily understood if the terms of equation (38) are regrouped. Let it be assumed that an arbitrarily chosen parameter,  $\alpha_{pl}$ , is to be varied so as to minimize error. Then an appropriate regrouping of equation (38) in terms of powers of  $\alpha_{pl}$  yields

$$\begin{aligned} \theta = & \left[ \int_0^T y^2(t) dt - 2 \sum_{\substack{i=1 \\ (i, m \neq l, p)}}^K \sum_{m=0}^L \alpha_{mi} \phi_{mi} + \sum_{\substack{i=1 \\ (i, m \neq l, p)}}^K \sum_{m=0}^L \sum_{\substack{j=1 \\ (j, n \neq l, p)}}^K \sum_{n=0}^L \alpha_{mi} \alpha_{nj} \phi_{minj} \right] \\ & + \left[ -2 \phi_{pl} + \sum_{\substack{i=1 \\ (i, m \neq l, p)}}^K \sum_{m=0}^L \alpha_{mi} \phi_{mip l} + \sum_{\substack{j=1 \\ (j, n \neq l, p)}}^K \sum_{n=0}^L \alpha_{nj} \phi_{p l n j} \right] \alpha_{pl} + [\phi_{plpl}] \alpha_{pl}^2 \quad (39) \end{aligned}$$

In this equation, the appearance of an inequality in parenthesis below a summation indicates exclusion of that double index from that summation. It is evident, from this regrouped expression, that the performance measure is a quadratic (nonrotated parabolic) function of the coefficient,  $\alpha_{pl}$ . A necessary expression for the coefficient  $\alpha_{pl}$  for which the critical values of the performance measure occur is obtained by equating the partial derivative of the performance measure with respect to  $\alpha_{pl}$  to zero; thus

$$\frac{\partial \theta}{\partial \alpha_{pl}} = 0 \quad (40)$$

Effecting the indicated differentiation of  $\theta$  yields

$$\alpha_{pl} = \frac{1}{\phi_{plpl}} \left( \phi_{pl} - \sum_{\substack{i=1 \\ (i, m \neq l, p)}}^K \sum_{m=0}^L \alpha_{mi} \phi_{mip l} \right) \quad (41)$$

or equivalently,

---

\*No attempt is made to orthogonalize equation (37) so as to simplify equation (38). Orthogonalization in the time-varying case is as difficult as obtaining the solution for the minimum. It is therefore of no value.

$$\sum_{i=1}^K \sum_{m=0}^L \alpha_{mi} \phi_{mip} = \phi_{pl} \quad (42)$$

Equation (41) shows that the value of  $\alpha_{pl}$  for which a single critical value of the performance measure (error) occurs is given by a linear combination of the other coefficients. Proceeding similarly yields a necessary expression for the critical value of each coefficient. A set of  $K(L+1)$  simultaneous linear algebraic equations with  $K(L+1)$  unknowns results:

$$\sum_{i=1}^K \sum_{m=0}^L \alpha_{mi} \phi_{mip} = \phi_{pl}; \quad \begin{aligned} p &= 0, 1, 2, \dots, L \\ l &= 1, 2, \dots, K \end{aligned} \quad (43)$$

It is seen that the solution for the constants, and therefore for the time-varying gains, is given by simultaneous linear algebraic equations, instead of simultaneous unstable boundary-value-differential equations, as in the calculus-of-variations approach.

Appendix B of this report consists of a proof that the solution of the above algebraic equations always yields a set of constants which produce the minimum value of the performance measure,  $\theta$ . Thus, the optimal value of  $\theta$  is given when the constants obtained from equations (43) are used. If the equations are linearly independent, a unique minimum exists. If they are linearly dependent, a single minimum value of error yet exists, but is given by a family of solutions, any one of which is satisfactory.

To ascertain that the critical value for each coefficient is a minimum, it must be shown that the second partial derivative with respect to each coefficient is greater than zero. (This condition insures that the parabolic function of each coefficient possesses a minimum.) The second partial derivative is

$$\frac{\partial^2 \theta}{\partial \alpha_{pl}^2} = 2\phi_{plpl} = 2 \int_0^T \beta_p^2(t) x_l^2(t) dt \quad (44)$$

If  $\beta_p(t)$  is zero only at isolated points in time and if the output of the  $l^{th}$  component filter is non-zero over some finite interval, then this second partial derivative is greater than zero. Accordingly, as long as each component filter has some output signal, a minimum exists for each coefficient, and is given by the solution of the equations of expression (43). Use will be made of this fact in describing the subsequent iteration method of solution.

Both a real-time and a non-real-time technique of characterization will be developed from the above concepts. The solution of the non-real-time algebraic equations will generally involve the determination of a large number

of constants,  $\alpha_{pl}$ 's. Consequently, close control of error propagation in the solution is essential. The previous mathematical development is sufficient to enable a straightforward derivation of a convergent iterative technique for the solution when the number of constants to be determined is large. A straightforward fast-running digital computer program can be written for use in effecting the actual solution.

Equation (41) yields the optimal value of  $\alpha_{pl}$  if all the other coefficients are fixed while  $\alpha_{pl}$  is being adjusted. This is the key to the convergent iterative procedure. Assume that an initial set of the coefficients is given, and then an arbitrary coefficient  $\alpha_{pl}(r)$  is changed to the value  $\alpha_{pl}(r+1)$  obtained from equation (41). If the new value is different from the initial value, the corresponding value of the measure of performance,  $\theta(r+1)$ , will be definitely less than the original value of the measure of performance,  $\theta(r)$ . This decrease in error results whether or not the equations of expression (43) are linearly independent. If the equations are dependent, the initial choice of the coefficients determines which single solution of the family is eventually obtained. Then, the next coefficient is changed according to its corresponding optimal condition equation. As long as the coefficients change by continuation of this process, the performance measure will decrease. If, by definition, an iteration cycle consists of the adjustment of each coefficient once, then as long as one or more coefficients change during each iteration cycle,  $r$ , the performance measure at the end of each cycle is monotone decreasing. Since the measure must be positive or zero, a lower bound exists. Consequently,  $\theta(r)$  is convergent as  $r$  approaches infinity.

It must now be shown that the coefficients do indeed change with each iteration cycle until the process converges to an optimal set of coefficients. If the coefficients do not change for an entire iteration cycle, then the set of equations of expression (43) has been satisfied. But if all of the equations are satisfied, an optimal solution (which was shown to be given by the solution of these equations) has been reached. Thus, the coefficients must change until an optimal solution is obtained.

Equation (38) yields the value of the performance measure,  $\theta$ , after any given number of iteration cycles. If the error is computed from time to time in the iteration process, the rate of convergence and final error can be determined.

The previous discussion has described in detail the fixed form approach as applied to the human-operator characterization problem. It is clear that this method always leads to a solution for the exact minimum of the properly specified (and constrained) problem. Indeed, the technique is practical, since linear simultaneous algebraic equations are involved, whose solution can always be obtained by an iterative technique. It has been shown that there is no possibility for solution instability; moreover, the solution must always converge to a unique value of minimum error.

The fixed-form method leaves an important question unanswered. Basically, the fixed-form method is a solution framework to which the particular time-varying characterization problem can be fitted. The question of the

choice of the fixed time functions  $\beta_m(t)$  is crucial, since these functions determine the type of constraint which is being specified. This constraint implicitly determines the compromise between error and time-variation of the gains. Moreover, it determines the amount and type of smoothing to be used along each axis in the detection of either the time-varying impulse response or time-varying transfer function (for the linear case). As a consequence of the influence of the constraint upon smoothing, both a non-real-time solution and a real-time solution can be developed. Both of these solutions will be discussed herein. In each case a particular set of constraining time functions will be chosen which appear to offer the most advantages in characterization.

### Non-Real-Time Solution

If it is assumed that both the human operator's entire input signal and the entire output signal are available in the interval  $0 \leq t \leq T$ , these data can be used so as to minimize the error between the output of the model and that of the human operator. As a consequence, one could expect smaller errors in the non-real-time case than in the real-time case, since instantaneous future information is available in the non-real-time case.

An important property which the fixed-time functions must possess in the non-real-time case is that they treat each point in the interval between 0 and  $T$  equally. In other words, no single point or interval should be weighted more heavily than another. Also of importance is the fact that the functions must limit the changes in the time-varying gains in an acceptable fashion. Lastly, it should be possible to change the fixed-time functions in a convenient way, so that the compromise between time-variation of the gains and error in characterization may be set at any reasonable level.

Experimental investigation has shown that a set of staggered triangular interpolation functions is quite adequate in satisfying the above requirements. These triangular functions are given by

$$\beta_m(t) = \begin{cases} 1 - |(t - m\frac{T}{L})| \frac{L}{T}; & (m-1)\frac{T}{L} \leq t \leq (m+1)\frac{T}{L} \\ 0; & \text{elsewhere} \end{cases} \quad (45)$$

where it is assumed that the interval of integration of the performance measure runs from  $t=0$  to  $t=T$ .

When weighted and added, these functions are capable of synthesizing the functions  $a_i(t)$ , which are then made up of connected straight-line segments. (See Fig. 2.)

Of course, the triangular fixed-time functions do not treat each point within the interval from  $t=0$  to  $t=T$  exactly equally. The synthesized

waveforms have discontinuous first derivatives at the points  $t = \frac{mT}{L}$ ;  $m=0, 1, 2, \dots, L$ . It appears that the only set of fixed-time functions which does treat each point in the interval equally is the finite set of Fourier series components with fundamental period of  $T$  seconds. However, the use of a finite Fourier series of fixed-time functions has the disadvantage of yielding a "Gibbs phenomenon", or ripple effect, which would, no doubt, be more detrimental than the effect of the discontinuous first derivative in the straight-line synthesis obtained with the triangular functions.

The use of the triangular functions affords a great advantage in the computation of the quantities,  $\phi_{minj}$ . If equation (45) is substituted into equation (37), the resulting equation is

$$\phi_{minj} = \int_0^T x_i(t) x_j(t) \left\{ \begin{array}{l} 1 - |(t - m\frac{T}{L})| \frac{L}{T} \\ 0 \end{array} \right\} \left\{ \begin{array}{l} 1 - |(t - n\frac{T}{L})| \frac{L}{T} \\ 0 \end{array} \right\} dt \quad (46)$$

where the left-hand bracketed quantity has value only in the interval

$$(m-1)\frac{T}{L} \leq t \leq (m+1)\frac{T}{L}$$

and the right-hand bracketed quantity has value only in the interval

$$(n-1)\frac{T}{L} \leq t \leq (n+1)\frac{T}{L}$$

Consequently,

$$\phi_{minj} = 0 \text{ when the integers } m \text{ and } n \text{ are such that } |m - n| \geq 2 \quad (47)$$

Equation (47) allows a great reduction in the number of averages that must be obtained. This reduction is very important because of the lengthy programs which are required to compute transfer characteristics.

The base length of the triangular fixed-time functions can be varied by changing the value of the integer,  $L$ . Consequently, the choice of the value of  $L$  determines the compromise which is reached between error in characterization and the amount of time-variation to be tolerated in the transfer characteristics.

It is certainly true that a wide variety of sets of fixed-time functions could have been chosen for synthesizing the time-varying gains. However, it appears that each set has some disadvantages, and therefore it is probably best to choose that set which has computational advantages. No doubt, if a set

of perfect fixed-time functions were available, their use in solution would be as difficult as solving the unstable boundary-value problem posed earlier.

The non-real-time approach is more suited for digital computation than it is for analog computation because of the storage capacity of digital computers. It is only necessary to read in the input record and output record of the human operator. The steps of the digital computation are the following:

- (1) The input record is filtered by digital filters which represent the chosen set of fixed component filters, thus producing the waveforms  $x_\ell(t)$ ,  $\ell = 1, 2, \dots, K$ .
- (2) The sets of functions  $\phi_{mi}$  and  $\phi_{minj}$  are computed. (This computation will require the choice of the integer,  $L$ , which determines the allowable variation in the time-varying gains.)
- (3) The algebraic equations which determine the values of the weighting gains,  $\alpha_{pl}$ , are solved by the iteration technique discussed previously.
- (4) These gains are used to compute the time-varying gains.
- (5) The time-varying gains are then used to compute the time-varying impulse response and time-varying transfer function over the interval.

#### Real-Time Solution

In the real-time solution to the optimal deterministic characterization problem, the performance measure and form of constraint must be modified somewhat. These modifications are dictated by the fact that the real-time problem is a two-axis (two independent variable) problem: the  $\lambda$  axis designates the running data axis and the  $t$  axis designates the present or real-time axis. The performance measure must be chosen such that no future values of data are required or, in other words, the upper limit of the integration over the variable  $\lambda$  must be  $t$ . Furthermore, it must be assumed that since each point  $\lambda$  will eventually be treated as the present time  $t$ , that the values of the time-varying gains can only be set at the present instant. In other words, one cannot go back into the past and readjust the gains, nor can one go forward of the present time and adjust the gains. Only the present values are free to be chosen. The present choice may, nevertheless, be based upon both present and past data. These requirements are all incorporated in the chosen performance measure, which is

$$\theta(t) \equiv \int_{-\infty}^t e^{\lambda} h(t-\lambda) d\lambda \quad (48)$$

where

$$e(\lambda) = y(\lambda) - \sum_{i=1}^K a_i(\lambda, t) x_i(\lambda) \quad (49)$$

In equation (48),  $h(\tau)$  is the impulse response of an arbitrary smoothing filter. In general, this filter should be chosen such that it weights present and recent past information most heavily, and eventually tapers the weighting to zero in the remote past. Equation (49) is the error equation in which the time-varying gains are assumed to be functions of both the running data and the present time. This notation for the time-varying gains may seem to be somewhat unusual; however, it places in clear view the effect of the constraint which is yet to be chosen. Moreover, it is certainly true that, in general, the gains are functions of the data involved and, since they change with time, are also functions of the present time. Accordingly, the two independent variables are appropriate.

In order to obtain a meaningful solution to the problem, it is again necessary to specify a constraint upon the gains  $a_i(\lambda, t)$ , because of the uncertainty principle. This constraint must be such that it maps the gains which are functions of two independent variables into functions of a single independent variable,  $t$ . In order to understand why the constraint must produce a function of the variable  $t$  only, the form of the performance measure with equation (49) substituted into equation (48) is considered. As long as  $a_i(\lambda, t)$  is allowed to be a function of both the variables  $\lambda$  and  $t$ , the solution is trivial, since the  $a_i$  can be chosen at each present instant, such that the performance measure is zero. Consequently, unless the constraint forces the gains to be functions of  $t$  only, the solution is trivial. In consideration of the above facts, the constraint to be chosen is the following

$$a_i(\lambda, t) = \alpha_i(t), \quad i = 1, 2, \dots, K \quad (50)$$

that is,  $a_i(\lambda, t)$  is to be constrained so as to be equal to a constant over  $\lambda$ , the constant being rechosen at each instant of present time,  $t$ .

It may seem that the original postulation of two-dimensional gains and the subsequent constraint which returns them to one-dimensional functions is a somewhat academic exercise. The justification for performing this group of steps is that a valid mathematical argument can be presented which places in evidence for the first time the effect of the uncertainty principle in the real-time problem. Moreover, the use of the performance measure and constraint as postulated above will now yield to an exact minimization procedure.

Upon carrying out the minimization procedure in a manner precisely analogous to the procedure used in the non-real-time solution, one obtains the result that the minimum value of the performance measure,  $\theta(t)$ , is obtained when

$$\sigma_{\ell}(t) = \sum_{i=1}^K \alpha_i(t) \sigma_{i\ell}(t); \quad \ell = 1, 2, \dots, K \quad (51)$$

where

$$\sigma_i(t) \equiv \int_{-\infty}^t x_i(\lambda) y(\lambda) h(t-\lambda) d\lambda \quad (52)$$

and

$$\sigma_{ij}(t) \equiv \int_{-\infty}^t x_i(\lambda) x_j(\lambda) h(t-\lambda) d\lambda \quad (53)$$

Once again, only the solution of algebraic equations is required. The equations vary with time and therefore must be re-solved at each instant. However, it is clear that the variable  $t$  is only a parameter in the solution.

It can be shown, as in the non-real-time case, that the solution of the algebraic equations yields a value of the performance measure which is less than, or equal to, the value for any other setting of the time-varying gains. Therefore, the minimum value of the performance measure is obtained at each instant of time,  $t$ .

The extreme ease with which the data,  $\sigma_i(t)$  and  $\sigma_{ij}(t)$  can be obtained makes this real-time solution highly practical. Fig. 3 is a diagram showing a physically realizable technique whereby  $\sigma_i(t)$  and  $\sigma_{ij}(t)$  may be computed by analog (or ordinary filtering) components.

The real-time solution has been obtained without specifying in detail the form of the smoothing filter, whose impulse response is given by  $h(\tau)$ . Thus, the information may be weighted in many different ways. The simplest and most easily realizable filtering operation is that obtained by use of a single low-pass filter. In this case,

$$h(\tau) = \begin{cases} e^{-\tau/\tau_0} & ; \tau \geq 0 \\ 0 & ; \tau < 0 \end{cases} \quad (54)$$

It can be realized by a single operational amplifier. If this form of filter is used, then  $\tau_0$  determines the compromise which is reached between error in solution and rapidity of variation in the time-varying gains. As  $\tau_0$  becomes larger, the gains vary slowly and the error is larger; and as  $\tau_0$  becomes small, the gains vary rapidly and the error becomes small.

It should be mentioned that the real-time solution has the advantage of having only one unknown in the algebraic equations for each time-varying gain.



At any instant of time, it is only necessary to solve linear algebraic equations with perhaps six unknowns. Of course, the equations must be re-solved at each instant of time. The fact that a relatively small number of unknowns exists in the real-time case is one of the advantages obtained by sacrificing knowledge of future information. Counterbalancing this advantage is the disadvantage that the real-time solution will produce somewhat larger errors than the non-real-time solution.

## EXPERIMENTAL VERIFICATION

An extensive experimental study was performed to verify and determine the usefulness of the previously described theory of deterministic characterization. The theory as described in this report is exact, and it is therefore only necessary to insure its correctness. An equally important goal is the determination of the usefulness of the techniques described for human-operator characterization. It is believed that both objectives were reached in this experimental study.

The experimental study consists of three main parts. They are:

- (1) Characterization of a known time-varying network whose transfer function is similar to that of the human operator. The time-varying network is operating in place of the human controller in a closed-loop control system, with an input signal which is similar to that encountered in man-machine systems. Both a non-real-time and a real-time characterization are performed. The system block diagram is shown in Fig. 4.
- (2) Characterization of a human pilot in one axis of a two-axis, closed-loop tracking task without motion cues. These data are taken from a NASA Langley simulation. In the non-real-time case, the trade-off between characterization error and time-variability of the transfer characteristic is adjusted and studied. In the real-time case, a single characterization is performed. The system block diagram is shown in Fig. 5.
- (3) Characterization of human operators in an interval of time during which an abrupt change in follow-up dynamics occurs. Half-way through the experiment, the follow-up system is changed so as to force the human operator to change his mode of tracking. Both non-real-time and real-time characterizations are performed over an interval which includes the change of mode. The system block diagram is shown in Fig. 6.

All of the processing of data was performed using a modern high-speed digital computer.\* However, the input data were obtained using analog computer equipment in combination with a display and control-stick arrangement. As stated earlier, in practice the non-real-time method is more suited to digital computation, and the real-time method is more suited to analog or special-purpose digital computation. However, the present study of both methods was performed on the digital computer so that advantage could be taken of the subroutines that are common to the two methods.

Solution of the algebraic equations for all non-real-time and real-time characterizations was performed by the iteration technique described in the previous section. The number of unknown coefficients varied from 7 in the real-time case up to a maximum of 105 in the non-real-time case. (The number of algebraic equations corresponds to the number of unknowns.) In every case the iteration process converged rapidly to the minimum error value (as predicted in theory), yielding the optimal set of coefficients. No instability or undesirable characteristics were noted, even though the iteration technique was used for approximately 1000 different sets of algebraic equations. Fig. 7 shows a typical plot of error in characterization versus number of iteration cycles for the real-time case (with 7 unknowns). Fig. 8 is typical of the error as a function of number of iteration cycles for the non-real-time case (with 91 unknowns). The rate of convergence was found to decrease slightly as the number of unknowns increased. However, in all cases the convergence is sufficiently fast to allow economical solution.

The choice of the fixed component filters is critical to the accuracy of the human operator characterization problem.\*\* These filters must be chosen such that the model corresponding to Fig. 1 is capable of accurately representing the human operator. Previous work in network and human operator characterization has shown that a set of so-called Kautz filters is capable of accurately characterizing the human operator.<sup>1</sup> They are given in transform by

$$H_i(j\omega) = \frac{\sqrt{2s_i}(j\omega - s_1)(j\omega - s_2) \cdots (j\omega - s_{i-1})}{(j\omega + s_1)(j\omega + s_2) \cdots (j\omega + s_{i-1})(j\omega + s_i)} \quad (55)$$

The constants,  $\sqrt{2s_i}$ , in the numerators are chosen so as to make the filters orthonormal over the semi-infinite time interval. However, since this property is not required in this deterministic theory, any convenient set of gains may be used, as long as they remain fixed throughout the entire characterization study. The poles  $s_1, s_2, \dots, s_K$  should be chosen so as to fall

---

\*This digital computer has a cycle time of 2.0 microseconds, and it had high speed input and output capabilities. The computer runs for the complete solution required from 5 to 12 minutes.

\*\*In this experimental study, only linear fixed-component filters were used.

within (and bracket) the region of the frequency axis in which the poles of the human operator are believed to lie. If the poles are logarithmically spaced, then minimum over-all characterization error will result.

In all these experiments, 7 fixed-component Kautz filters were used. The poles were set at the values 1.50, 2.31, 3.56, 5.48, 8.44, 12.99, and 20.01 radians per second, which are logarithmically related.

An initial computer run was made to determine whether the characterization was more accurate with the order of the poles increasing in frequency (starting with  $\mathcal{S}_1 = 1.50$  rad/sec) or with the order of the poles decreasing in frequency (starting with  $\mathcal{S}_7 = 20.01$  rad/sec). It was found that the error in characterizing a fixed-linear network similar in character to a human operator was the same for both runs. Accordingly, it was concluded that the usual pole order (increasing in frequency) was satisfactory. The ratio of the integral squared error to the integral squared output signal of the fixed network was found to be 0.000715. Thus, the error was extremely small.

In all of the experiments, the input (or disturbance) signal to the control system was generated by low-pass filtering of the output of a wideband noise generator. The low-pass filtering operation was varied slightly from one experiment to the next, as indicated by the power spectral densities given in Figs. 4, 5, and 6.

All experiments except those specifically noted were performed over 1.0 minute of tracking data. In all cases, both the human operator (or substitute network), as well as the characterizing filters, were allowed to reach a "steady-state" tracking condition directly preceding the taking of data for the computation interval. In other words, both the human operator and the networks possessed memory of the signal prior to  $t = 0$ . This procedure for taking data made it possible to avoid a characterization transient due to warm-up immediately following  $t = 0$ .\*

In all non-real-time characterization runs, the triangular interpolation functions described by equation (45) were used. The integer,  $L$ , was varied so as to adjust the compromise between error in characterization and time-variability of the transfer characteristic. For the real-time case, the same smoothing filter was used for all runs. The filter used has the impulse response

$$h(\tau) = \begin{cases} 1 - \frac{\tau}{5.0} & ; 0 \leq \tau \leq 5.0 \text{ sec.} \\ 0 & ; \tau < 0 \text{ and } \tau > 5.0 \text{ sec.} \end{cases} \quad (56)$$

---

\* This deterministic theory could be used to study "warm-up" characteristics of the human operator at the beginning of a tracking task. It would only be necessary to take data under the condition that the input signal is zero prior to  $t = 0$ .

which is triangular. This filter was used because it is very easy to implement on the digital computer and because its weighting of past data eventually decreases to zero. The results obtained using this filter will be very similar to those obtained using a single time-constant filter (equation (54) ).

In all cases, visual presentation of the transfer characteristics is in terms of a special time-varying step response. It was supposed that there is no need to deal with the human operator's time-varying transfer function in this experimental study because the conversion from impulse response to transfer function is straightforward and requires no verification. On the other hand, the time-varying impulse response does not lend a great deal of intuitive insight. Consequently, a special step response characteristic was developed, which does lend insight and is easily computed. This special step response is given by

$$s(t, \tau) = \int_{-\infty}^{\tau} h(t, \tau_1) d\tau_1, \quad (57)$$

where  $h(t, \tau)$  is the time-varying impulse response as defined earlier. This special step response is not generally equal to the true step response of the network whose impulse response is  $h(t, \tau)$ . In order to use the function  $s(t, \tau)$  for computation of the network response to an arbitrary signal,  $s(t, \tau)$  should be partially differentiated with respect to  $\tau$  and then used in equation (1).

Lastly, it should be mentioned that a special technique was used to simulate the Kautz fixed-component filters digitally. A method attributed to Tustin was employed, which allows the accurate simulation of a continuous filter by a digital difference equation.\* With this technique, it was only necessary to use a rate of 10 samples per second for the human operator's input and output waveforms. It will be recalled that the highest frequency among the poles of the Kautz filters is 20.01 radians per second or 3.2 cycles per second. The sampling theorem therefore requires that a minimum sampling rate of 6.4 samples per second be used. It will be seen that the Tustin method is indeed efficient, since it does yield good results even when the theoretical minimum sampling rate is approached.

## Results of Experiment 1

In this experiment, the objective was to determine the accuracy with which the non-real-time and the real-time characterization techniques could characterize a known, time-varying linear network which is somewhat similar

---

\*A discussion of the problem of digital simulation of continuous filtering operations is given in Reference 17.

to the transfer function of the human operator. (See Fig. 4.) In order to avoid the problem of energy decay within the network to be characterized when a time change in that network is made, the signal  $y(t)$  was obtained by switching among the outputs of three filters. In this way definite, abrupt step changes along the time axis of the network to be characterized could be realized. Fig. 9 is an isometric plot of the theoretical special step response of the network to be characterized. The three constant networks are consecutively switched into the output,  $y(t)$ , for 20 seconds during the data run.

The non-real-time characterization was computed with the constant,  $L$ , set equal to 12. Thus, the interval between the peaks of the triangular fixed-time function, called the data interval, was 5 seconds per interval. It was found that the percent normalized integral squared error (100 times the ratio of the integral of the squared error signal to the integral of the squared value of the desired signal,  $y(t)$  when the optimal characterization network was used was 1.79%, with the great majority of the error occurring at the two abrupt step changes. The isometric plot of the special step response for the optimal non-real-time characterization is shown in Fig. 10. This plot clearly demonstrates the ability of the non-real-time technique to accurately characterize the known time-varying network. It is seen that the greatest part of the inaccuracy occurs at the abrupt change in the network being characterized. However, it is unlikely that the human operator would undergo time changes as severe as those shown in Fig. 9. Consequently, this characterization is an extreme test of the non-real-time technique.

The real-time characterization was also successful. The percent normalized integral squared error for the optimal characterization filter was 7.53%. This larger error value can be attributed to the fact that in the real-time characterization future information cannot be used. Fig. 11 is an isometric plot of the special step response for the optimal real-time characterization filter. This plot is somewhat deceiving, because it does not exhibit the special step response within the intervals along the  $t$  axis. There are errors which do not appear on the plot in the fifth interval ( $20 < t \leq 25$ ) and in the ninth interval ( $40 < t \leq 45$ ); that is, those intervals immediately following the abrupt changes in the known filter. Nevertheless, there is very little error elsewhere. Fig. 11 demonstrates the ability of the real-time technique to accurately characterize the known time-varying network.

## Results of Experiment 2

This experiment was designed so as to allow characterization of the human pilot in one axis of a two-axis task and to allow study of the compromise or uncertainty between error in characterization and rapidity of time variation of the characterization model. The data were obtained at NASA, Langley Research Center, for a well-practiced pilot, by Mr. James J. Adams and his associates.

In the non-real-time case, the integer,  $L$ , was varied over a wide range of values. In order to avoid excessively high processing costs for

large values of  $\Delta$  (rapid time variation, small error), the data interval was shortened. In all cases, the beginning of the data interval was the same point. Table I summarizes the pertinent information and results of the various characterizations. The uncertainty or compromise between error in characterization and time-variability is clearly demonstrated. The fourth column represents the error in characterization, and the first column represents the degree of variability. As the number of intervals per minute increases (indicating greater allowed variability), the characterization error decreases. Fig. 12 is a plot of this uncertainty as represented by error versus data interval. The case in which the data interval is 60 seconds per interval is very nearly the same as that which assumes the transfer characteristic is constant. The error for constant coefficients would be approximately 37.0%.

Figs. 13 through 17 are isometric plots of the characterized special step response for the pilot under various settings of the data interval. All of the plots start at the same point in the data run, but several are not presented for the entire 60 seconds for reasons of economy, as stated earlier. It is evident, from the plots, that greater variability is obtained as the data interval decreases.

An interesting incidental discovery was made while working with this experiment and Experiment 3. It appears that the human operator often exhibits a nonminimum phase transfer characteristic. This characteristic, which is sometimes assumed to be a pure delay, causes the step response of the characterization model to begin with a negative-going transient. In order to be sure that the human operator's response is indeed more like a nonminimum phase network than like a network with pure delay, a computer optimal characterization run was made with a 0.1-second delay incorporated in the characterization filter.\* It was found that a 20% increase in error occurred, thus indicating a poorer approximation for the pure delay case.\*\*

While the experimental verification was in progress, a new analog output facility was connected to the digital computer. This equipment is capable of plotting the special step responses for the optimal characterization networks. Consequently, the remaining portion of the experimental verification was performed using this plotting equipment. It was necessary, however, to discontinue the isometric presentation and to have the special step responses plotted serially. In all of the remaining special step response

---

\* The characterization filter was optimized with the pure delay incorporated. Thus, the best filter for use with a 0.1-second delay was obtained.

\*\* After all the experiments had been completed, a known nonminimum phase network was characterized by the non-real-time method. The resulting error was very small and the response of the model was almost identical to that of the known network. This experiment served as another check upon the above stated results.

TABLE I  
Summary of Information and Results  
For the Non-Real-Time Case of Experiment 2

Effective Value of L (Intervals/Min.)	Actual Value of L	Data Run Length, T (Sec.)	% Norm. Int. Sq. Error	Data Interval (Secs./Interval)	Spec. Step Response Plotted in
1	1	60	36.4%	60.0	Fig. 13
6	6	60	34.0	10.0	Fig. 14
12	12	60	21.5	5.0	Fig. 15
24	12	30	9.4	2.5	Fig. 16
60	14	14	2.99	1.0	Fig. 17

records, the running time is upward from the lower left corner. When the top of a column is reached, the continuation is at the bottom of the next column to the right.

The real-time portion of Experiment 2 shows a similar type of special step response to that obtained for the non-real-time case. (See Fig. 18.) A considerable degree of time variability is present, and there are approximately three different characteristic responses which appear repetitively. The percent normalized integral squared error is 42.07%.

### Results of Experiment 3

The objective of Experiment 3 was to determine the ability of the characterization methods to accurately characterize a forced change in the human operator's mode of tracking. This change was initiated by making a significant change in the follow-up dynamics at the exact midpoint in time of the data interval. (See Fig. 6.) Data were taken for four subjects, each of whom had practiced for a short time with each of the two sets of dynamics. The first subject was a test pilot, experienced in variable-stability aircraft. The second was an engineering student. The third and fourth were research engineers. The numerical results of the characterization experiment are given in Table II.

In the non-real-time case, the integer  $L$  was set equal to 12 for all runs, thus producing a data interval of 5 seconds per interval.

Both the non-real-time and the real-time special step responses for the optimal characterizations exhibit marked changes as functions of time. (See Figs. 19 through 26.) In all cases, the special step response is relatively constant in running time up to the time,  $t = 30$  seconds. The significant change occurs in the neighborhood of  $t = 30$  seconds, and then the special step responses settle to new characteristic responses. It is quite clear that the change in tracking mode of each human operator resulting from changed dynamics has been detected. Once again the nonminimum phase character of the human operator over parts of each record is evident.

It was found that the subjects tracked the error signal in significantly different ways. Subject 2 used rather violent corrective stick motions, subjects 1 and 3 used more or less average corrective motions, and subject 4 used very mild corrective measures. The special step response plots for the various subjects show the manifestations of these various modes. Subject 2 possesses a special step response which has a high gain and very little lag, whereas the response of subject 4 has low gain and significant lag.



TABLE II  
Characterization Results for Experiment 3

Subject No.	Occupation	<sup>*</sup> % N.I.S.E., Non-Real-Time	% N.I.S.E., Real-Time	Non-Real-Time Step Response Plotted in	Real-Time Step Response Plotted in
1	Pilot	4.94%	18.63%	Fig. 19	Fig. 23
2	Student	13.20%	39.19%	Fig. 20	Fig. 24
3	Engineer	6.61%	28.32%	Fig. 21	Fig. 25
4	Engineer	3.90%	9.10%	Fig. 22	Fig. 26

<sup>\*</sup>Normalized integral squared error.

## CONCLUSIONS

The optimal deterministic characterization theory presented in this report has been experimentally verified. It has been shown that it is possible to obtain time-varying transfer characteristics in a practical manner by using an exact theory of constrained fixed-form optimization. When a special iteration technique is used in combination with the fixed-form theory, stability within the solution for the characterization filter yielding minimum error is always assured. In every practical case, there is a unique value of minimum error, and it must be given when the optimal characterization filter is used.

An uncertainty in characterization is demonstrated which requires that a compromise be reached between the error in characterization and the time-variability of the optimal time-varying transfer characteristic. It has also been shown that both the non-real-time and the real-time characterization techniques are capable of detecting changes in the time-varying transfer characteristic of the human operator.

Cornell Aeronautical Laboratory, Inc.  
Of Cornell University  
Buffalo, New York, November 16, 1964.

## APPENDIX A

### MATHEMATICAL SYMBOLS

$J$	a kernel function of a nonlinear network
$K$	an integer equal to the number of component filters in the characterization model
$L$	an integer which is one less than the number of fixed-time functions used.
$T$	the length of time in seconds of the characterization interval
$f$	a function representing a general integrand
$i, j, l, m, n, p, q$	general integers
$r$	an integer representing the number of an iteration cycle in the minimization process.
$t$	independent variable, time, in seconds
$\theta$	performance measure representing the amount of error in characterizing the human operator
$\lambda$	variable of integration; "data" axis time variable (seconds)
$\tau, \tau_i$	independent variables representing lags in time (seconds)
$H_i(j\omega)$	transfer function of a network whose impulse response is $h_i(\tau)$
$H(t, j\omega)$	time-varying transfer function of a network whose time-varying impulse response is $h(t, \tau)$
$\mathcal{H}(j\omega, j\omega)$	bifrequency transfer function of a time-varying linear network whose time-varying impulse response is $h(t, \tau)$
$J_i$	kernel function of a nonlinear component filter of a model filter
$s_i$	pole or zero of a fixed linear component filter in a model filter
$S(t, \tau)$	special step response of a linear time-varying network whose impulse response is $h(t, \tau)$
$X(j\omega)$	Fourier transform of $x(t)$

$Z(j\omega)$	Fourier transform of $z(t)$
$N_n$	a class of nonlinear networks, the class becoming more inclusive as $n$ increases
$a_i(t)$	time-varying gain weighting the signal $x_i(t)$
$b_i(t)$	general time-varying gain
$e(t)$	error in characterizing the human operator
$g_i(\tau)$	general impulse response of a fixed linear network
$h(\tau)$	linear weighting function used in computing $\bar{x}_i(t)$ and $\bar{x}_{ij}(t)$
$h_i(\tau)$	impulse response of a component filter of a model filter
$h(t, \tau)$	impulse response of a time-varying linear network
$x(t)$	input signal; signal considered as the input to a display which a human operator is tracking
$x_i(t)$	output of a component filter of a model filter
$y(t)$	output of the human operator; desired output of the characterization model filter
$z(t)$	output of a linear or nonlinear network
$\theta_\ell$	non-real-time integral of the product of $y(t)$ and $x_\ell(t)$
$\theta_{i\ell}$	non-real-time integral of the product of $x_i(t)$ and $x_\ell(t)$
$\theta(t)$	instantaneous performance measure representing the amount of error in characterizing the human operator in the real-time case
$\alpha_i(t)$	constrained time-varying gain in the real-time solution
$\alpha_{m\ell}$	a constant which is used to weight the fixed-time function,
$\beta_{m\ell}(t); \beta_m(t)$	one of a group of fixed-time functions which are weighted so as to make up the time-varying gains,
$\bar{x}_i(t)$	short-time weighted average of the product of $y(t)$ and $x_i(t)$
$\bar{x}_{ij}(t)$	short-time weighted average of the product of $x_i(t)$ and $x_j(t)$

$\lambda^2$	arbitrary positive constant representing relative weighting in a calculus-of-variations problem
$ju$	a second Fourier frequency variable
$\phi_{mi}, \phi_{minj}$	non-real-time averages of data required for minimization of the performance measure, $\theta$
$\tau_o$	time-constant of an exponential weighting function
$j\omega$	a first Fourier frequency variable

A dot over a symbol indicates a derivative with respect to the corresponding independent variable.

## APPENDIX B

### PROOF THAT A SOLUTION OF THE ALGEBRAIC EQUATIONS (43) YIELDS A SET OF COEFFICIENTS FOR THE CHARACTERIZATION MODEL WHICH PRODUCES MINIMUM ERROR

Substitution of equations (43) into equation (38) yields the optimal value of the performance measure

$$\theta_{OPT} = \int_0^T y^2(t) dt - \sum_{i=1}^K \sum_{m=0}^L \alpha_{mio} \phi_{mi} \quad (1b)$$

where the  $\alpha_{mio}$ 's are the solutions obtained from equations (43). Suppose that a different set of constants are used instead of those obtained from equations (43). These non-optimal constants,  $\alpha_{mi}$ , could be written as

$$\alpha_{mi} = \alpha_{mio} + \Delta_{mi} \quad (2b)$$

where each  $\Delta_{mi}$  is an arbitrary real constant. The value of the performance measure for the non-optimal coefficients,  $\alpha_{mi}$ , can be written as

$$\begin{aligned} \theta_{N.OPT} = & \int_0^T y^2(t) dt - 2 \sum_{i=1}^K \sum_{m=0}^L (\alpha_{mio} + \Delta_{mi}) \phi_{mi} \\ & + \sum_{i=1}^K \sum_{m=0}^L \sum_{j=1}^K \sum_{n=0}^L (\alpha_{mio} + \Delta_{mi})(\alpha_{njo} + \Delta_{nj}) \phi_{minj} \end{aligned} \quad (3b)$$

In order to show that the equations (43) will produce the minimum value of error, it must be shown that

$$\theta_{N.OPT} \geq \theta_{OPT} \quad \text{for any arbitrary sequence of numbers, } \Delta_{mi}, \quad (4b)$$

$$i = 1, 2, \dots, K; \quad m = 0, 1, 2, \dots, L$$

The following is a proof of inequality 4b.

Consider that

$$\int_0^T \left[ \sum_{i=1}^K \sum_{m=0}^L \Delta_{mi} \phi_m(t) x_i(t) \right]^2 dt \geq 0 \quad (5b)$$

since the integrand is always greater than or equal to zero. The integrand can be expanded such that the following condition is obtained:

$$\int_0^T \sum_{i=1}^K \sum_{m=0}^L \sum_{j=1}^K \sum_{n=0}^L \Delta_{mi} \Delta_{nj} \beta_m(t) \beta_n(t) x_i(t) x_j(t) dt \geq 0 \quad (6b)$$

which, from equation (37), is seen to be equivalent to

$$\sum_{i=1}^K \sum_{m=0}^L \sum_{j=1}^K \sum_{n=0}^L \Delta_{mi} \Delta_{nj} \phi_{minj} \geq 0 \quad (7b)$$

Consider also that, from the optimal values of the coefficients given by equations (43), it follows that

$$\sum_{i=1}^K \sum_{m=0}^L \Delta_{pl} \alpha_{mio} \phi_{mip l} = \Delta_{pl} \phi_{pl} \quad (8b)$$

$$\sum_{i=1}^K \sum_{m=0}^L \sum_{l=1}^K \sum_{p=0}^L \Delta_{pl} \alpha_{mio} \phi_{mip l} = \sum_{l=1}^K \sum_{p=0}^L \Delta_{pl} \phi_{pl} \quad (9b)$$

and therefore

$$\sum_{i=1}^K \sum_{m=0}^L \sum_{j=1}^K \sum_{n=0}^L \Delta_{nj} \alpha_{mio} \phi_{minj} - \sum_{j=1}^K \sum_{n=0}^L \Delta_{nj} \phi_{nj} = 0 \quad (10b)$$

Similarly, it can be shown that

$$\sum_{i=1}^K \sum_{m=0}^L \sum_{j=1}^K \sum_{n=0}^L \Delta_{mi} \alpha_{njo} \phi_{minj} - \sum_{i=1}^K \sum_{m=0}^L \Delta_{mi} \phi_{mi} = 0 \quad (11b)$$

Upon addition of equations (10b) and (11b) to inequality (7b), one obtains

$$\begin{aligned}
 & -2 \sum_{i=1}^K \sum_{m=0}^L \Delta_{mi} \phi_{mi} + \sum_{i=1}^K \sum_{m=0}^L \sum_{j=1}^K \sum_{n=0}^L \Delta_{mi} \alpha_{njo} \phi_{minj} \\
 & + \sum_{i=1}^K \sum_{m=0}^L \sum_{j=1}^K \sum_{n=0}^L \Delta_{nj} \alpha_{mio} \phi_{minj} + \sum_{i=1}^K \sum_{m=0}^L \sum_{j=1}^K \sum_{n=0}^L \Delta_{mi} \Delta_{nj} \phi_{minj} \geq 0
 \end{aligned} \tag{12b}$$

If  $\theta_{opt}$  is added to each side of inequality (12b), the left-hand side becomes equal to  $\theta_{N, opt}$ . Therefore, inequality (4b) is true, and the desired proof has been obtained.



## REFERENCES

1. Elkind, J.I., Starr, E.A., Green, D.M., and Darley, D.L., "Evaluation of a Technique for Determining Time-Invariant and Time-Variant Dynamic Characteristics of Human Pilots," NASA Tech. Note D-1897, Washington, D.C., May 1963.
2. Potts, T.F., Ornstein, G.N., and Clymer, A.B., "The Automatic Determination of Human and Other Parameters," Proc. Western Joint Computer Conf., May 1963 (Los Angeles, Calif.), pp. 645-660.
3. Adams, J.J., and Bergeron, H.P., "Measured Variation in the Transfer Function of a Human Pilot in Single Axis Tasks," NASA Tech. Note D-1952, October 1963.
4. Sheridan, T.B., "Time-Variable Dynamics of Human Operator Systems," M.I.T. Dyn. Anal. and Contr. Lab. Rept. R-124, March 1960.
5. Gardner, M.F., and Barnes, J.L., Transients in Linear Systems, Vol. 1, John Wiley and Sons, Inc., New York 1942, pp. 262-263.
6. Zadeh, L.A., "Frequency Analysis of Variable Networks," Proc. Inst. of Radio Engr., Vol. 38, March 1950, pp. 291-299.
7. Gersho, A., "Characterization of Time-Varying Linear Systems," Proc. I.E.E.E., Vol. 51, January 1963, (Correspondence), p. 238.
8. Kautz, W.H., "Transient Synthesis in the Time Domain," I.R.E. Trans. on Circuit Theory, Vol. CT-1, September 1954, pp. 29-39.
9. Huggins, W.H., "Representation and Analysis of Signals, Part I: The use of Orthogonalized Exponentials," A.F. Cambridge Research Center, TR 57-357, Bedford, Mass., September 1957.
10. Zadeh, L.A., "Optimum Nonlinear Filters," Journal of Appl. Phys., Vol. 24, No. 4, April 1953, pp. 396-404.
11. Heisenberg, W., The Physical Principles of the Quantum Theory, Dover Publications, Inc., New York, 1930.
12. Gabor, D., "Theory of Communication," Journal I.E.E., Vol. 93, Pt. 3, 1946, pp 429-457.
13. Wierwille, W.W., "A New Approach to the Spectrum Analysis of Nonstationary Signals," I.E.E.E., Trans. on Applications and Industry, No. 69, November 1963, pp. 322-327.
14. Weinstock, R., Calculus of Variations with Applications to Physics and Engineering, McGraw-Hill Book Co., New York, 1952, Ch. 3.

15. Wierwille, W.W., and Heckman, D.W., "Synthesis of Fixed-Form Nonlinear Filters," I.S.A. Trans., Vol. 3, July 1964, pp. 210-216.
16. Shannon, C.E., "Communication in the Presence of Noise," Proc. Inst. of Radio Engrs., Vol. 37, January 1949, pp. 10-21.
17. Fryer, W.D., and Schultz, W.C., "A Survey of Methods for Digital Simulation of Control Systems," Cornell Aeronautical Laboratory Report No. XA-1681-E-1, July 1964.

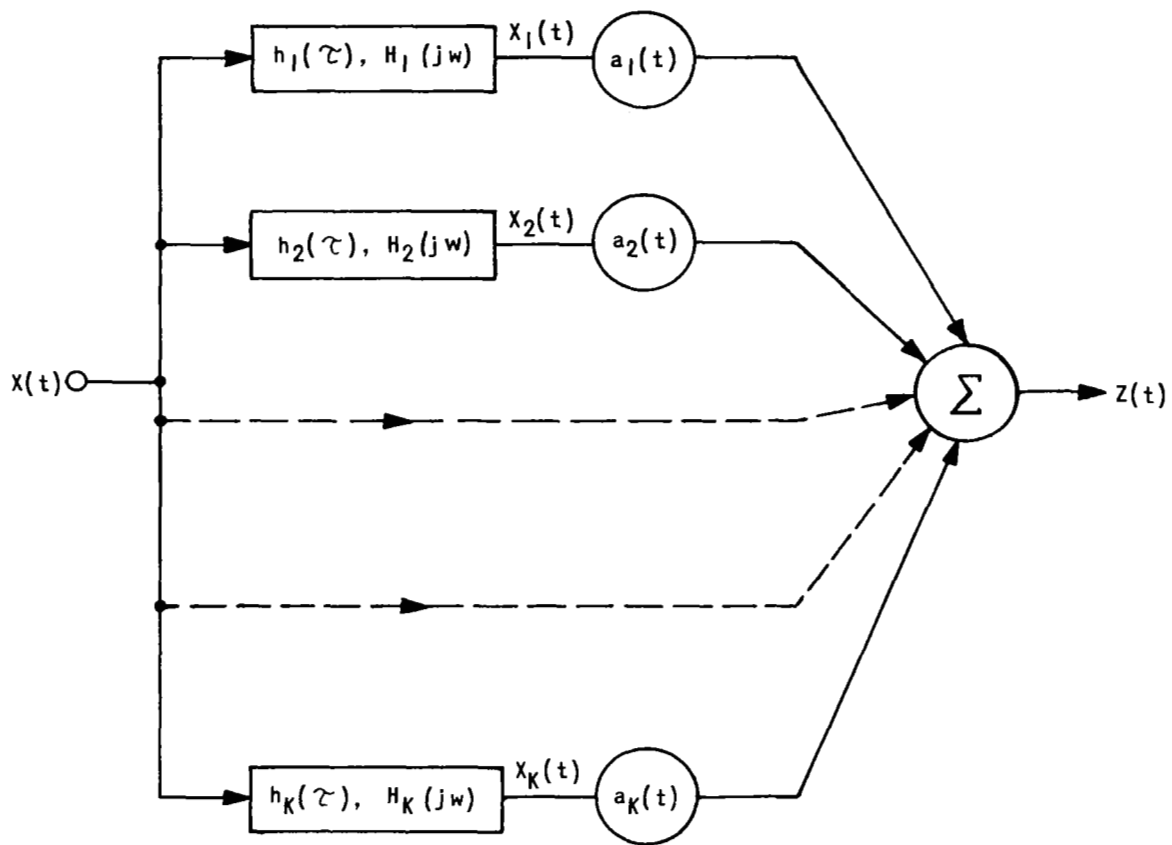


Figure 1 A network whose time-varying transfer function can be written in the form of equation (15).

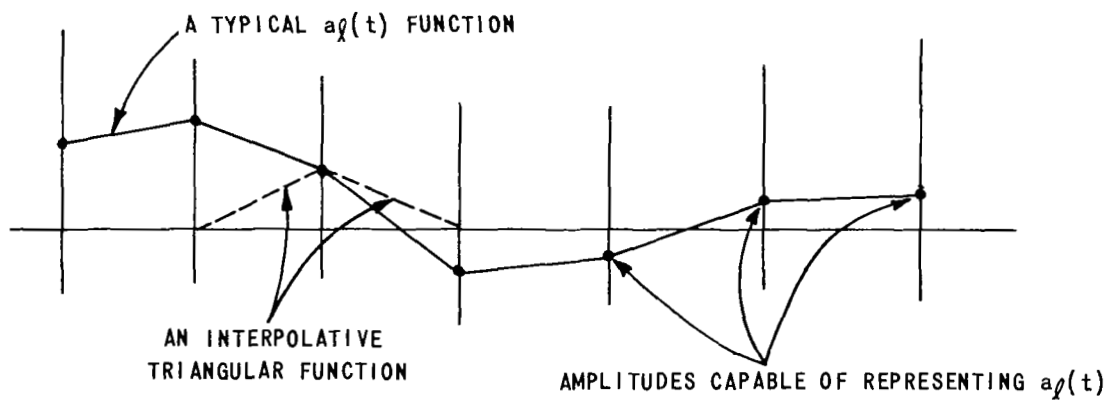


Figure 2 Graph of a typical time-varying gain using the staggered triangular functions as fixed time functions.

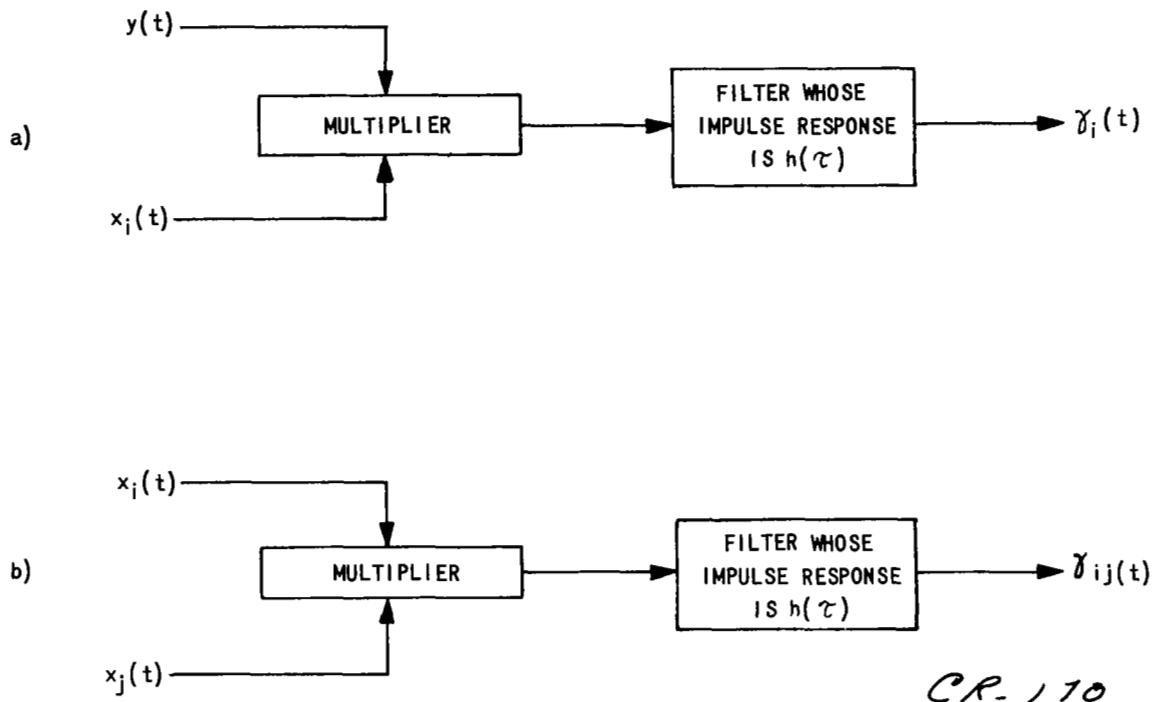


Figure 3 Diagram of equipment required for computing a)  $\gamma_i(t)$  and b)  $\gamma_{ij}(t)$

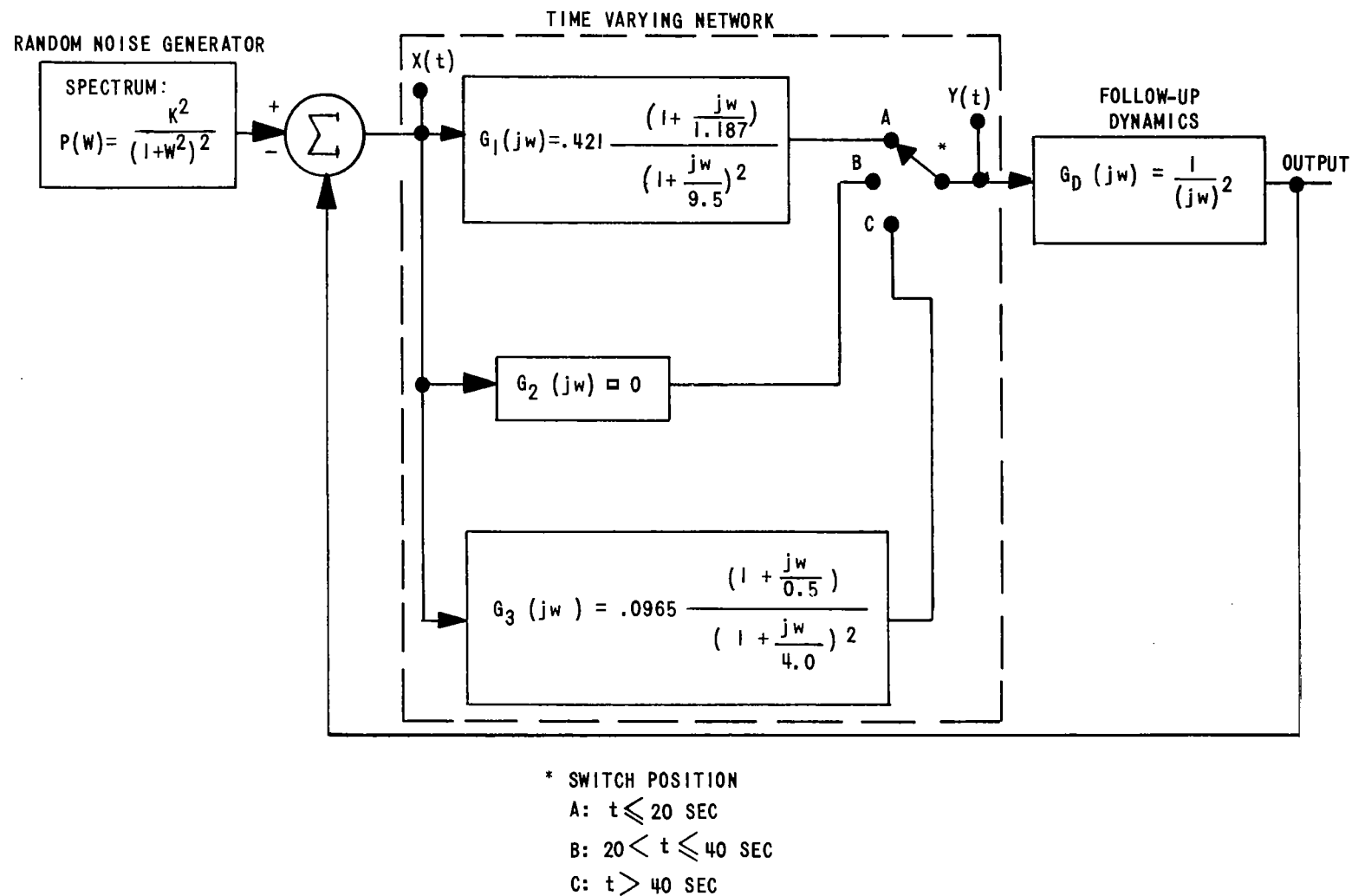


Figure 4 System block diagram used for characterization of known time-varying network, (Experiment 1).

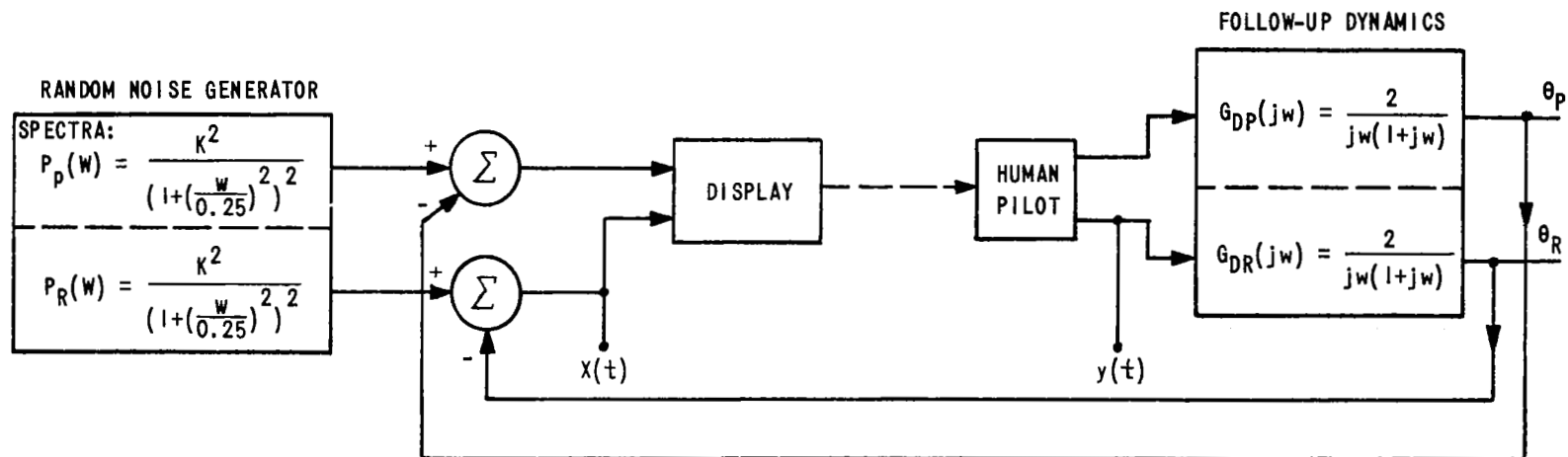


Figure 5 System block diagram used for characterization of human pilot in one axis of a two-axis task, (Experiment 2).

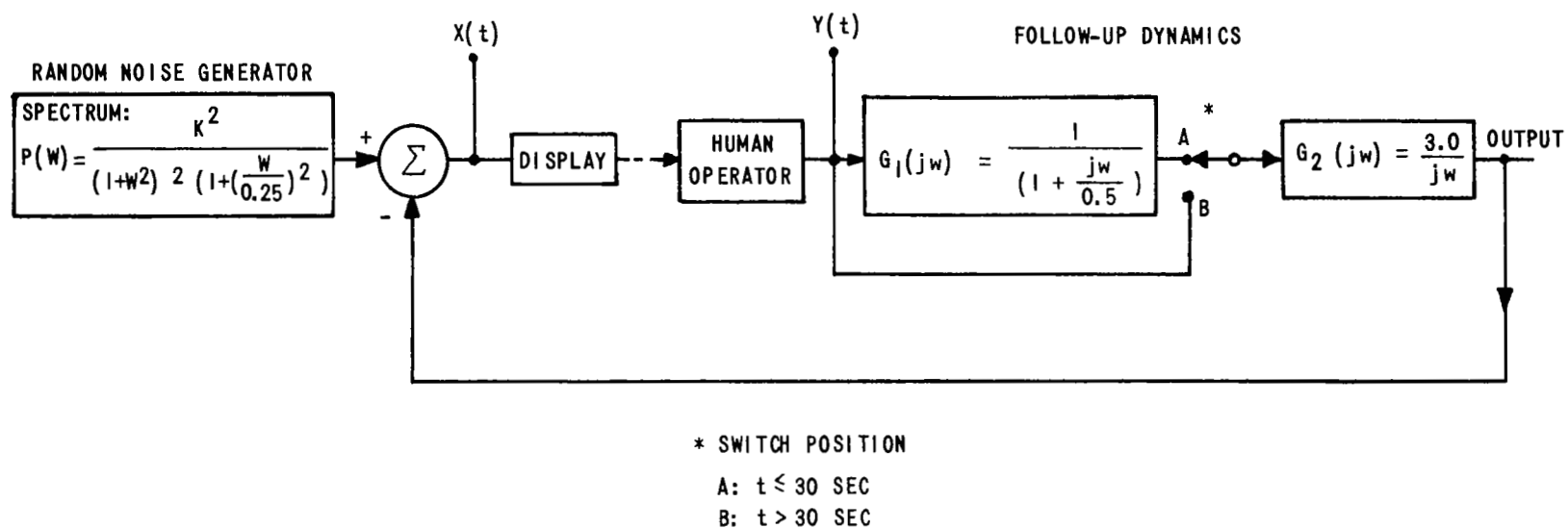


Figure 6 System block diagram for characterization of human operator during change of dynamics, (Experiment 3).



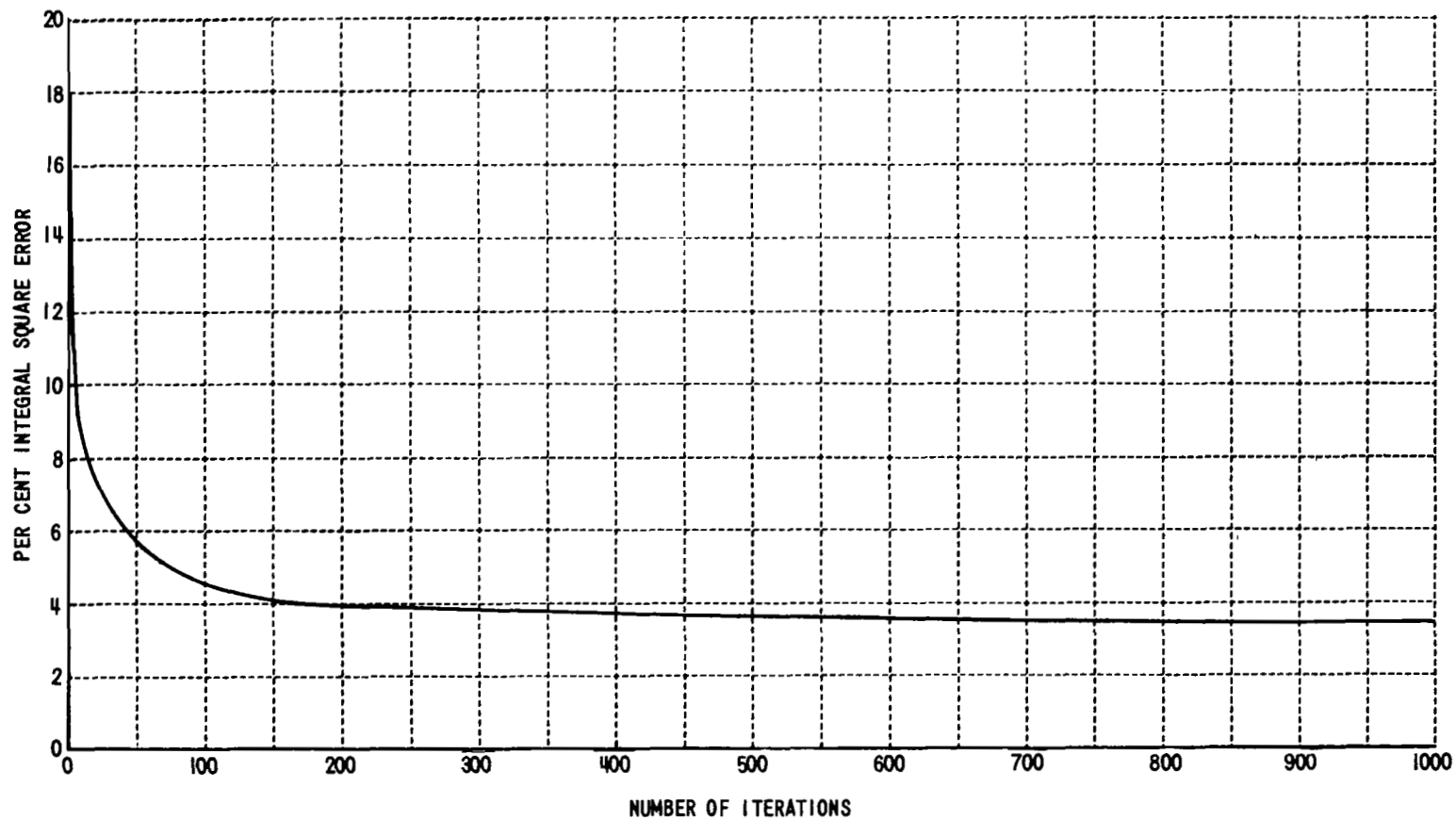


Figure 7 Typical plot of percent error in characterization versus number of iteration cycles for the real-time case (7 unknowns).

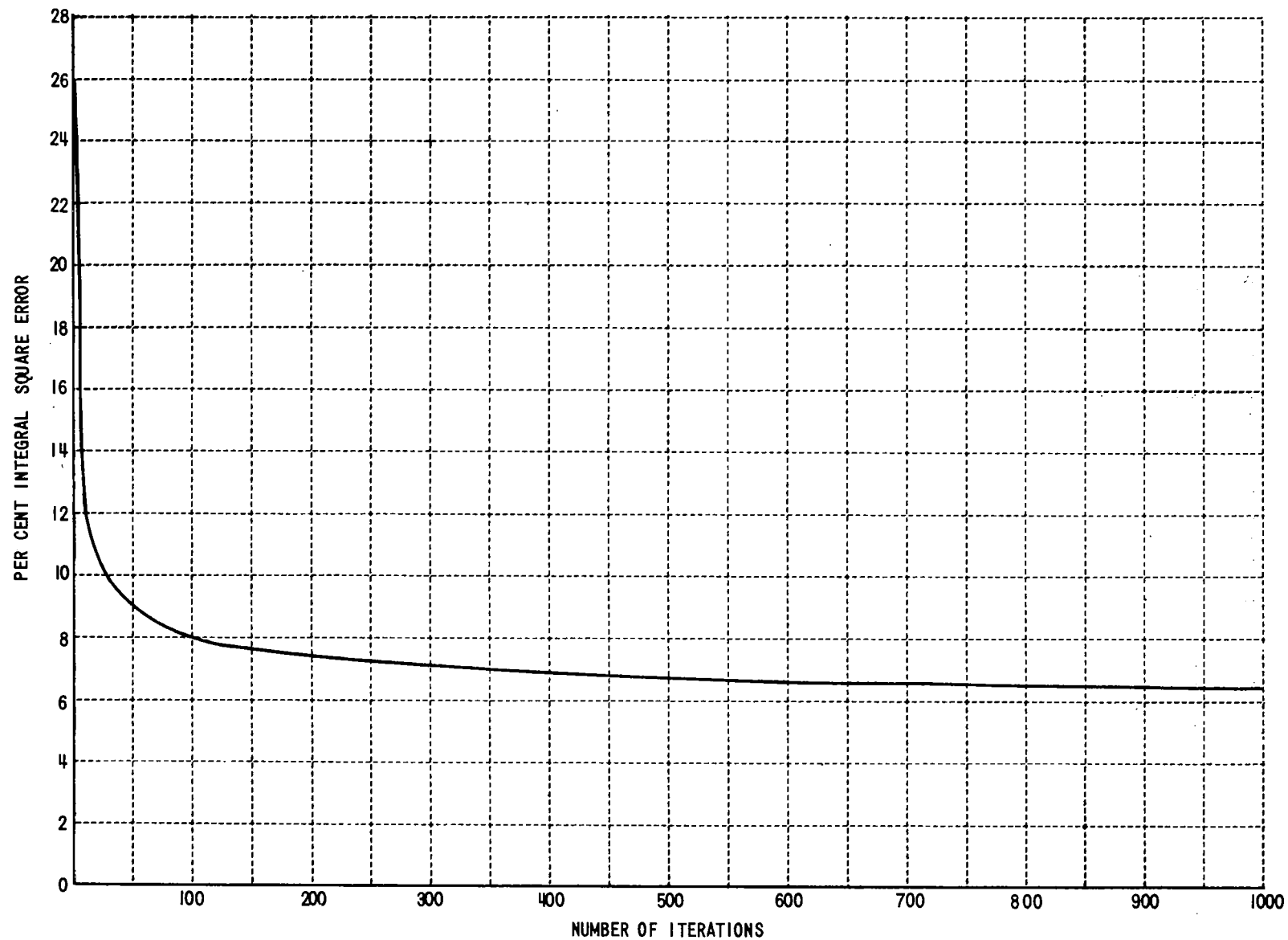


Figure 8 Typical plot of percent error in characterization versus number of iteration cycles for the non-real-time case (91 unknowns).

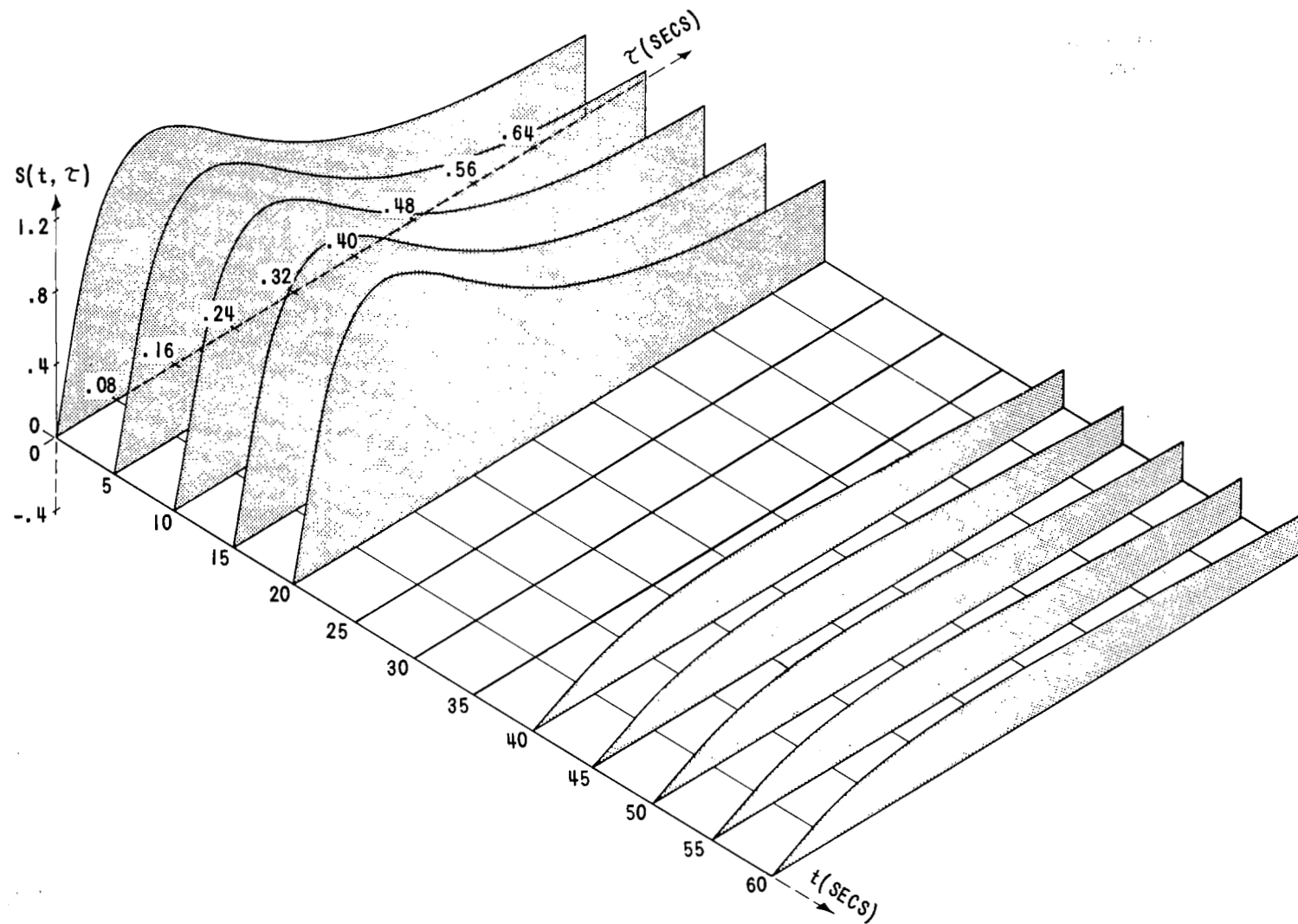


Figure 9 Isometric plot of the special step response of the known time-varying network to be characterized.

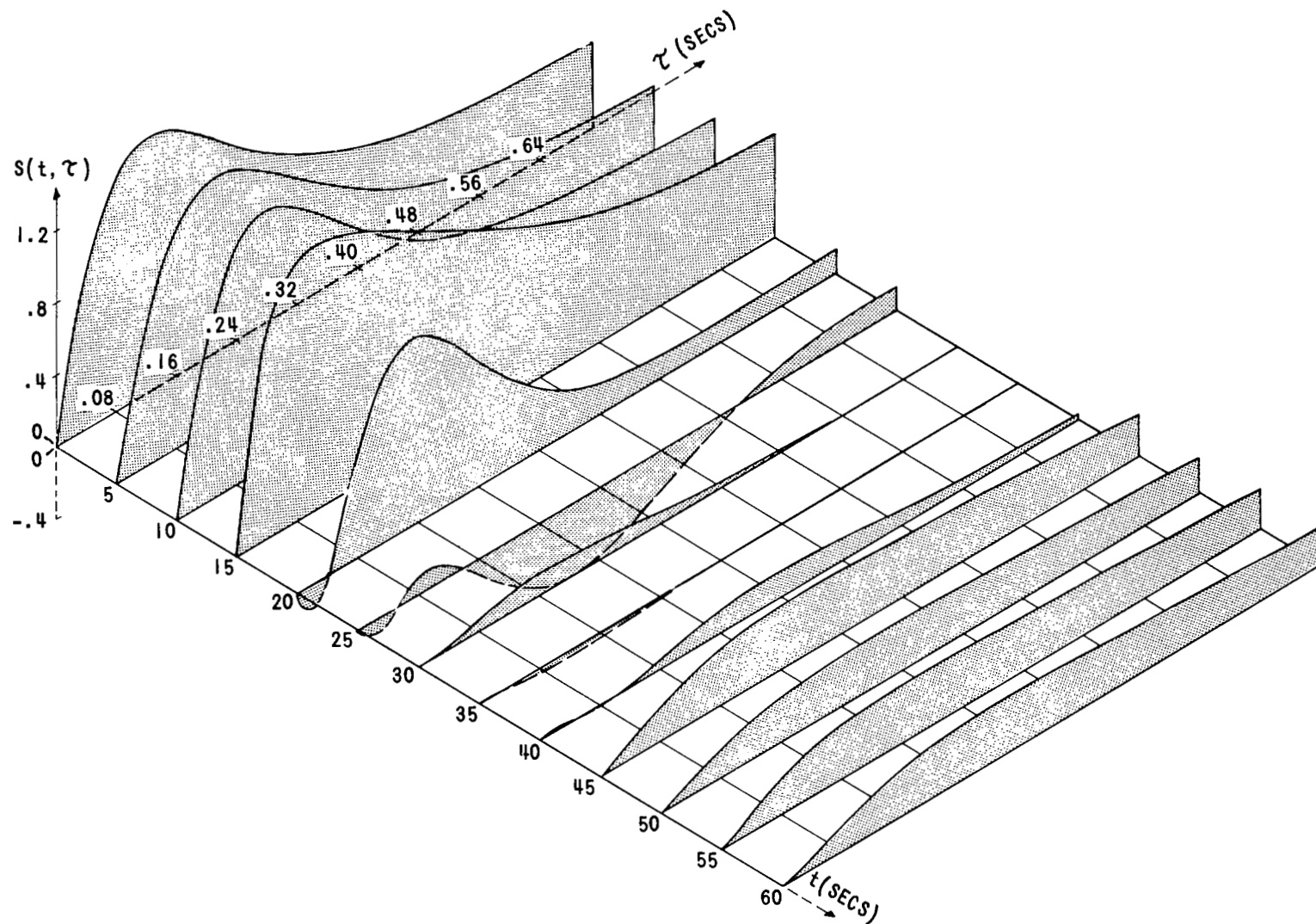


Figure 10 Isometric plot of the special step response for the optimal non-real-time characterization of the known, time-varying network.

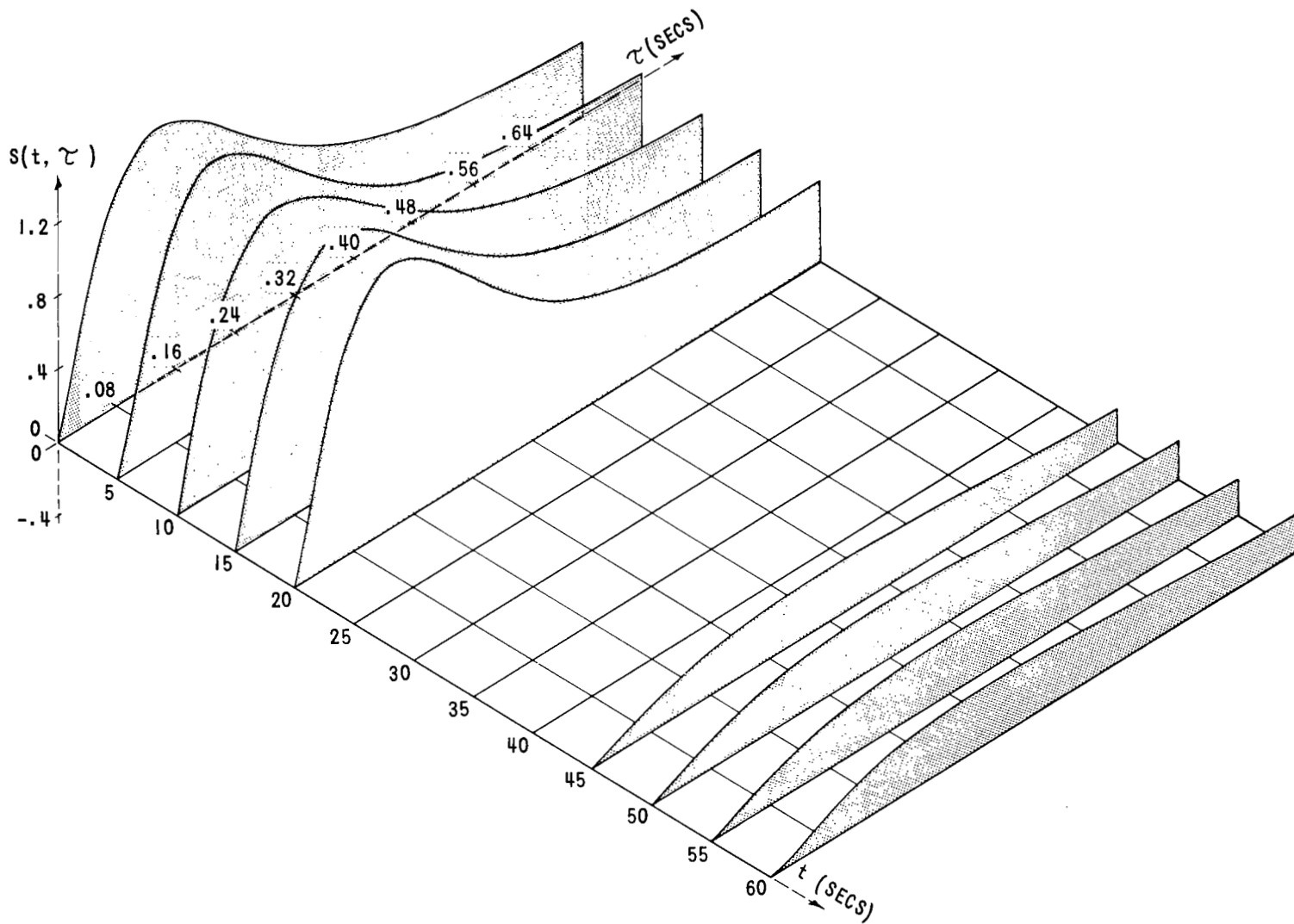


Figure 11 Isometric plot of the special step response for the optimal real-time characterization of the known, time-varying network.

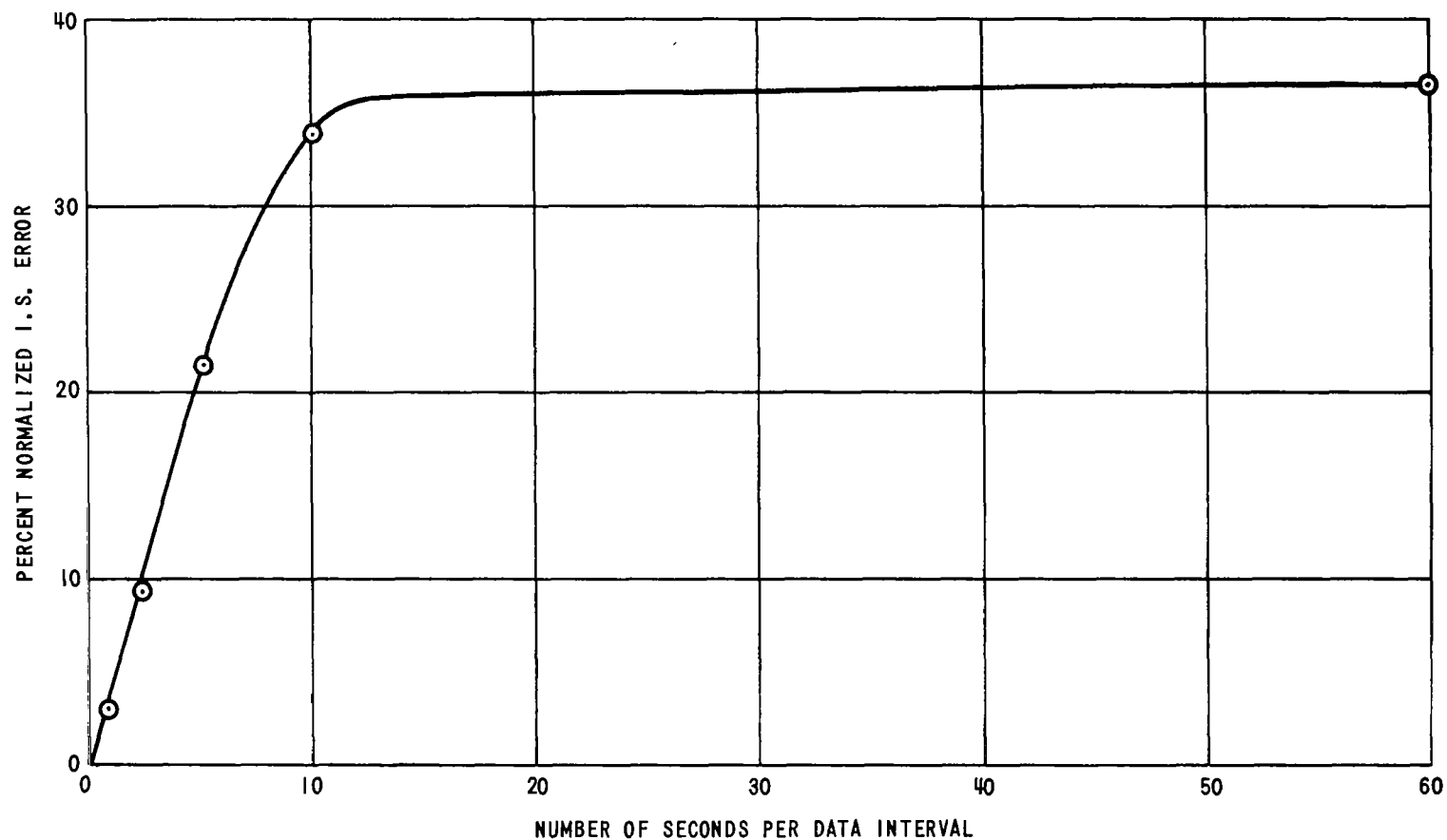


Figure 12 Graph of experimental data showing the compromise between error and variability of the transfer characteristic.

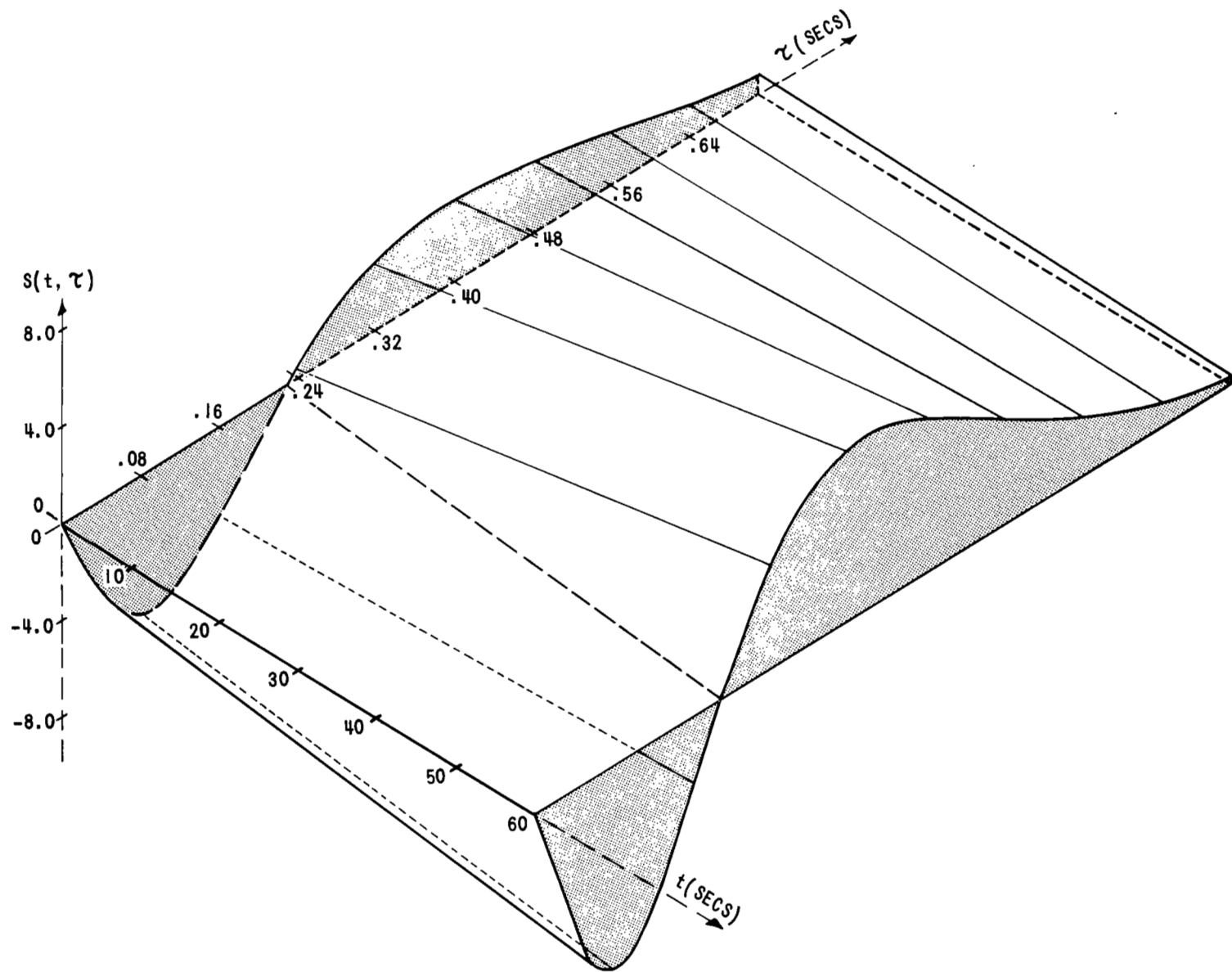


Figure 13 Isometric plot of non-real-time special step response of pilot characterization model (NASA data) for data interval = 60 sec/int.

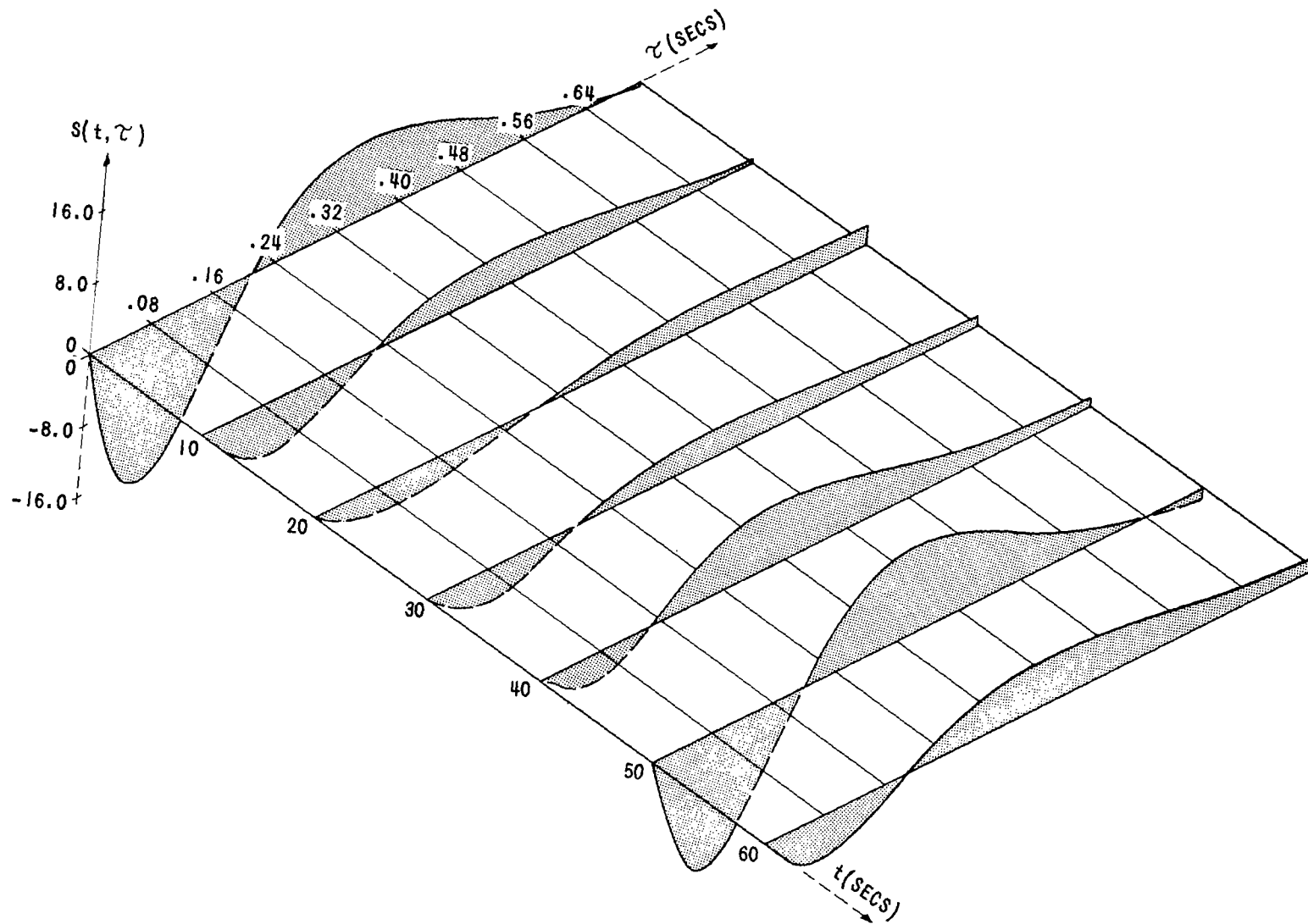


Figure 14 Isometric plot of non-real-time special step response of pilot characterization model (NASA data) for data interval = 10 sec/int.



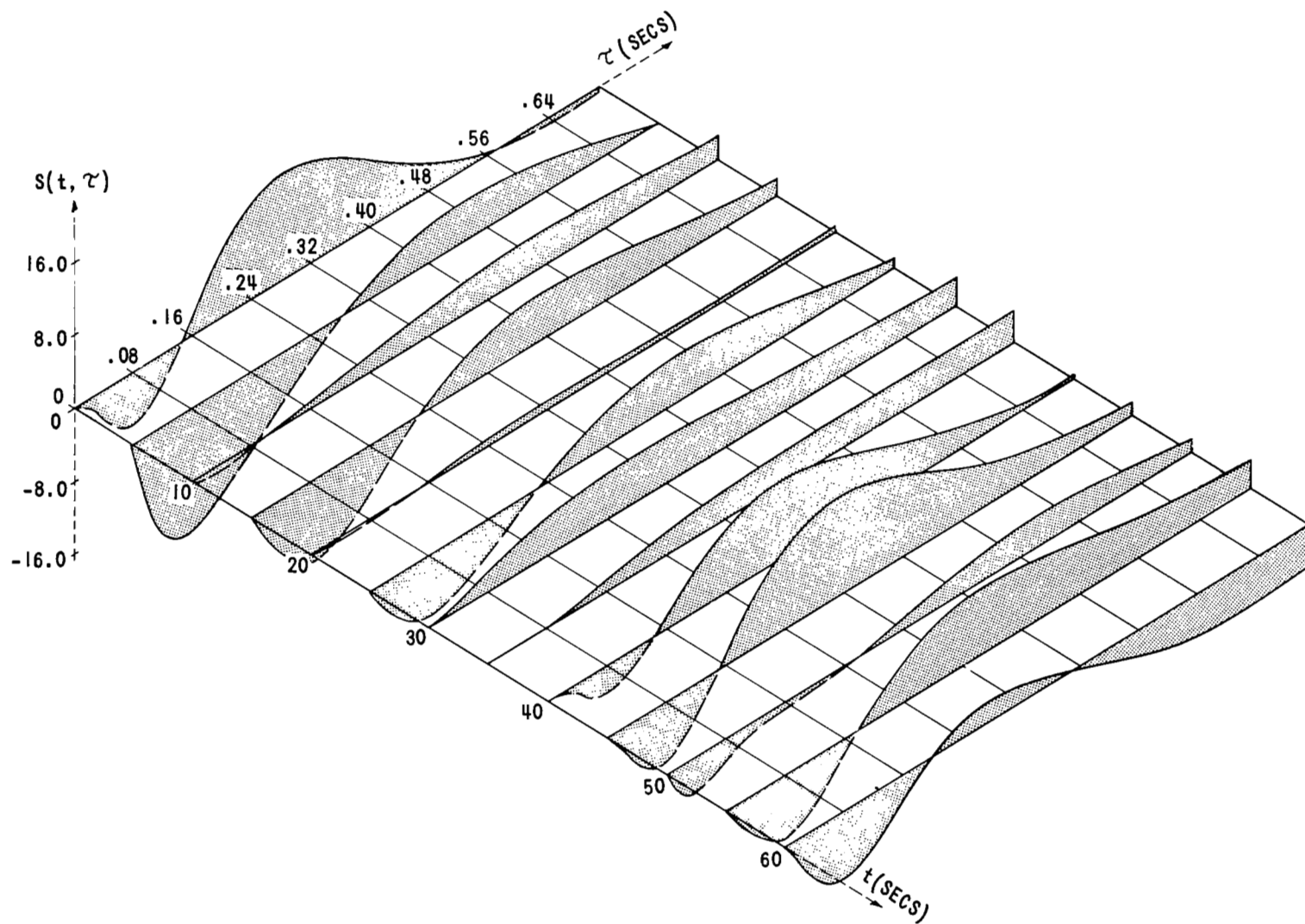


Figure 15 Isometric plot of non-real-time special step response of pilot characterization model (NASA data) for data interval = 5 sec/int.

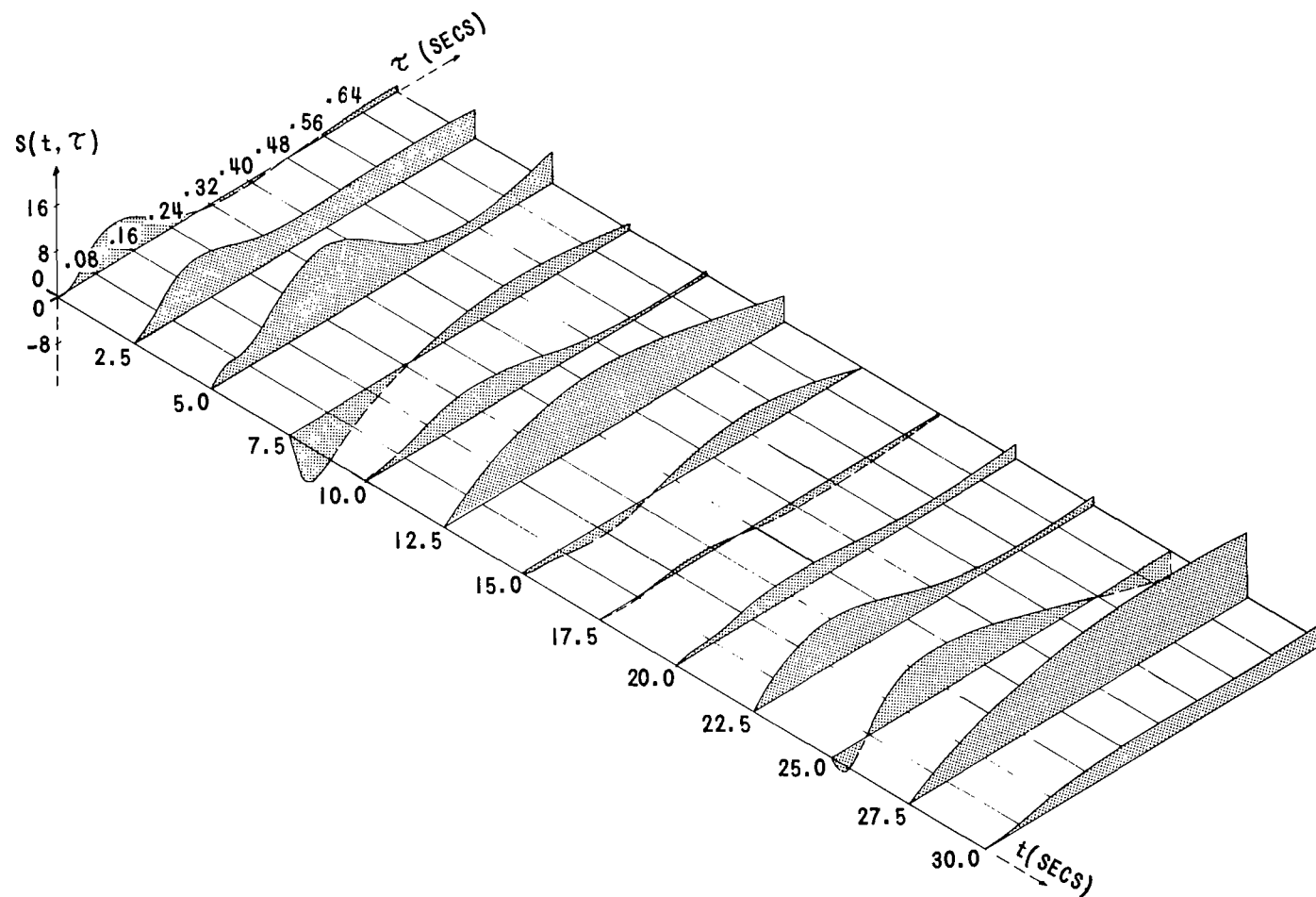


Figure 16 Isometric plot of non-real-time special step response of pilot characterization model (NASA data) for data interval = 2.5 sec/int.

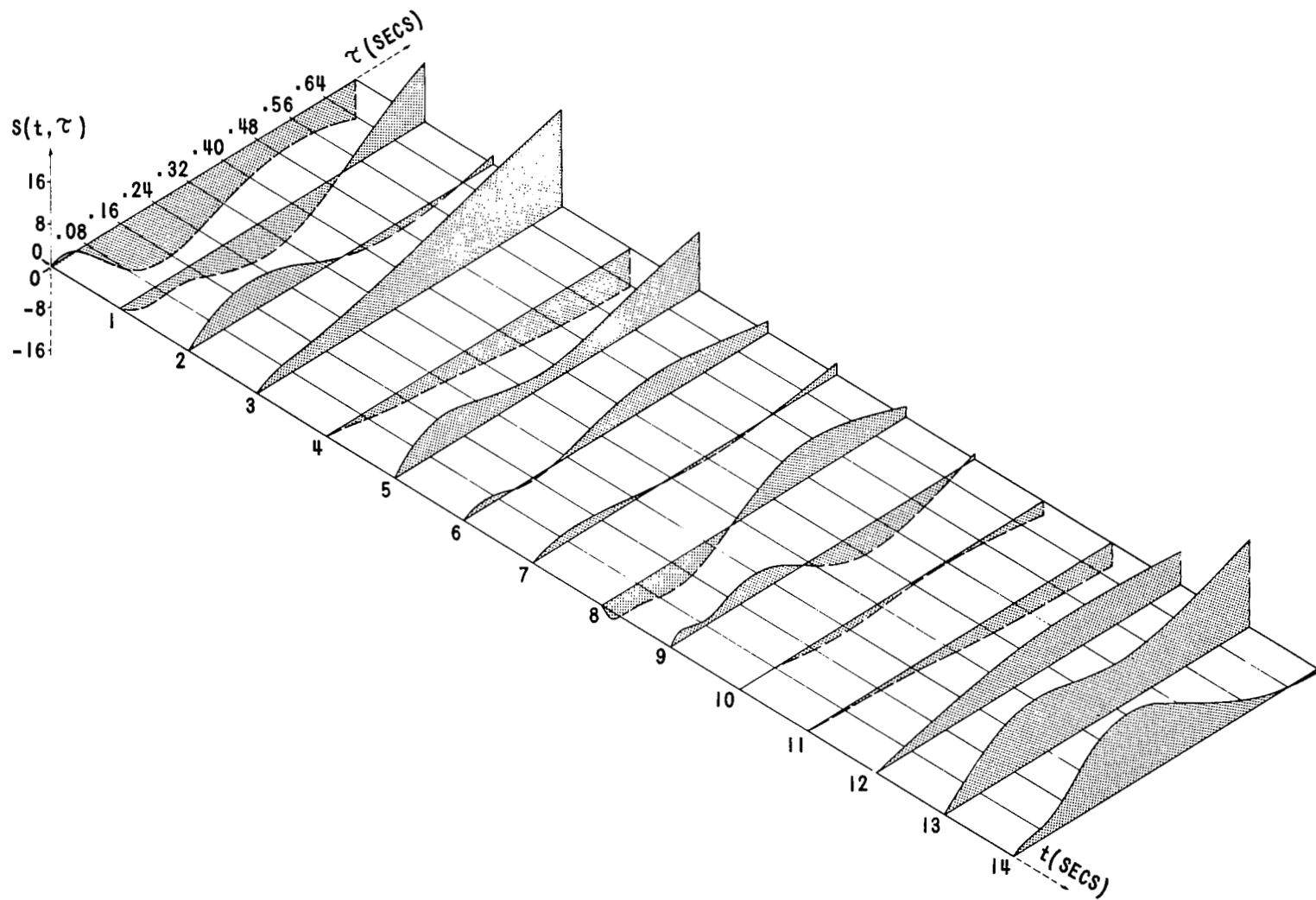


Figure 17 Isometric plot of non-real-time special step response of pilot characterization model (NASA data) for data interval = 1.0 sec/int.

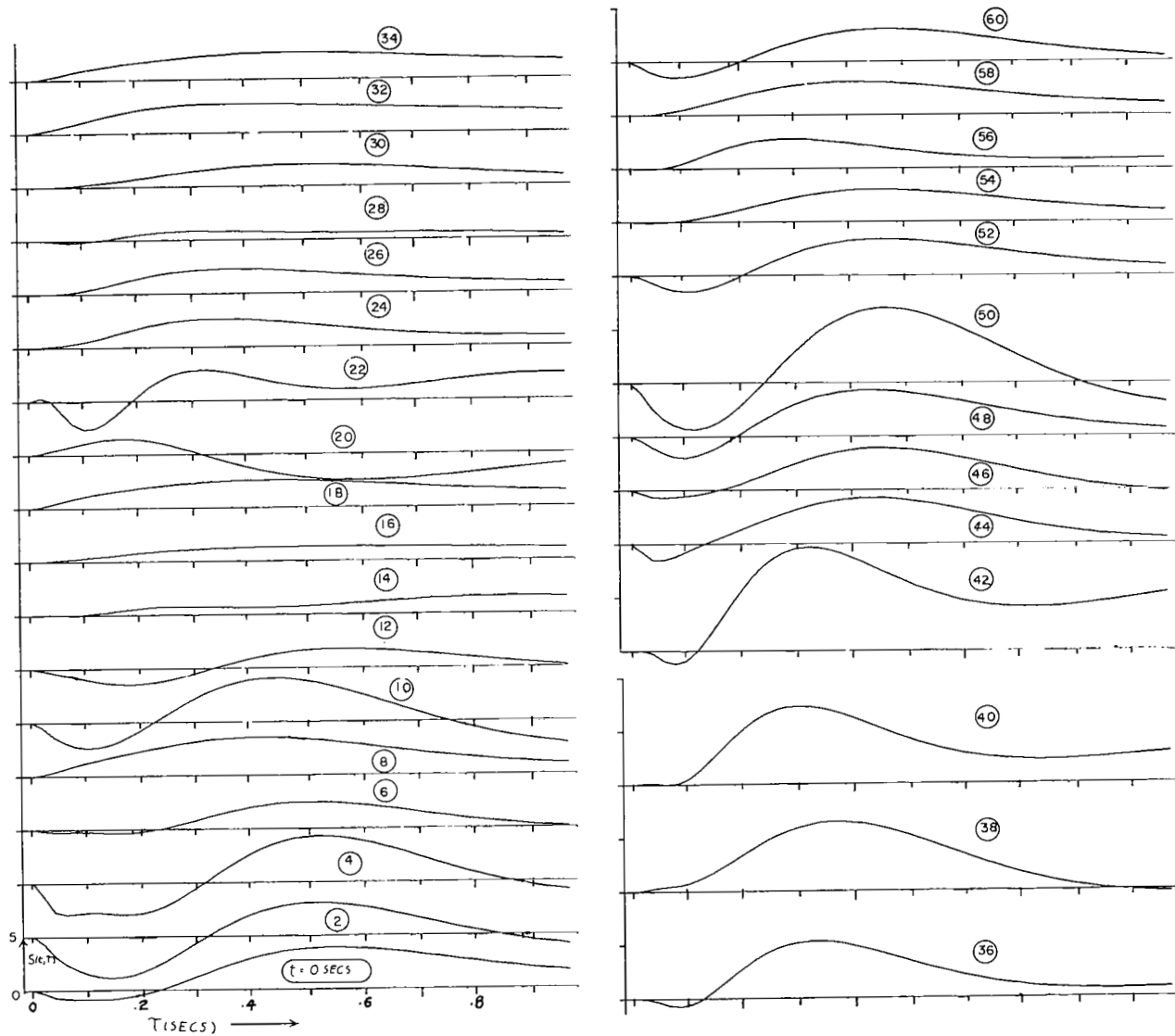


Figure 18 Plot of real-time special step response of pilot characterization model (NASA data).

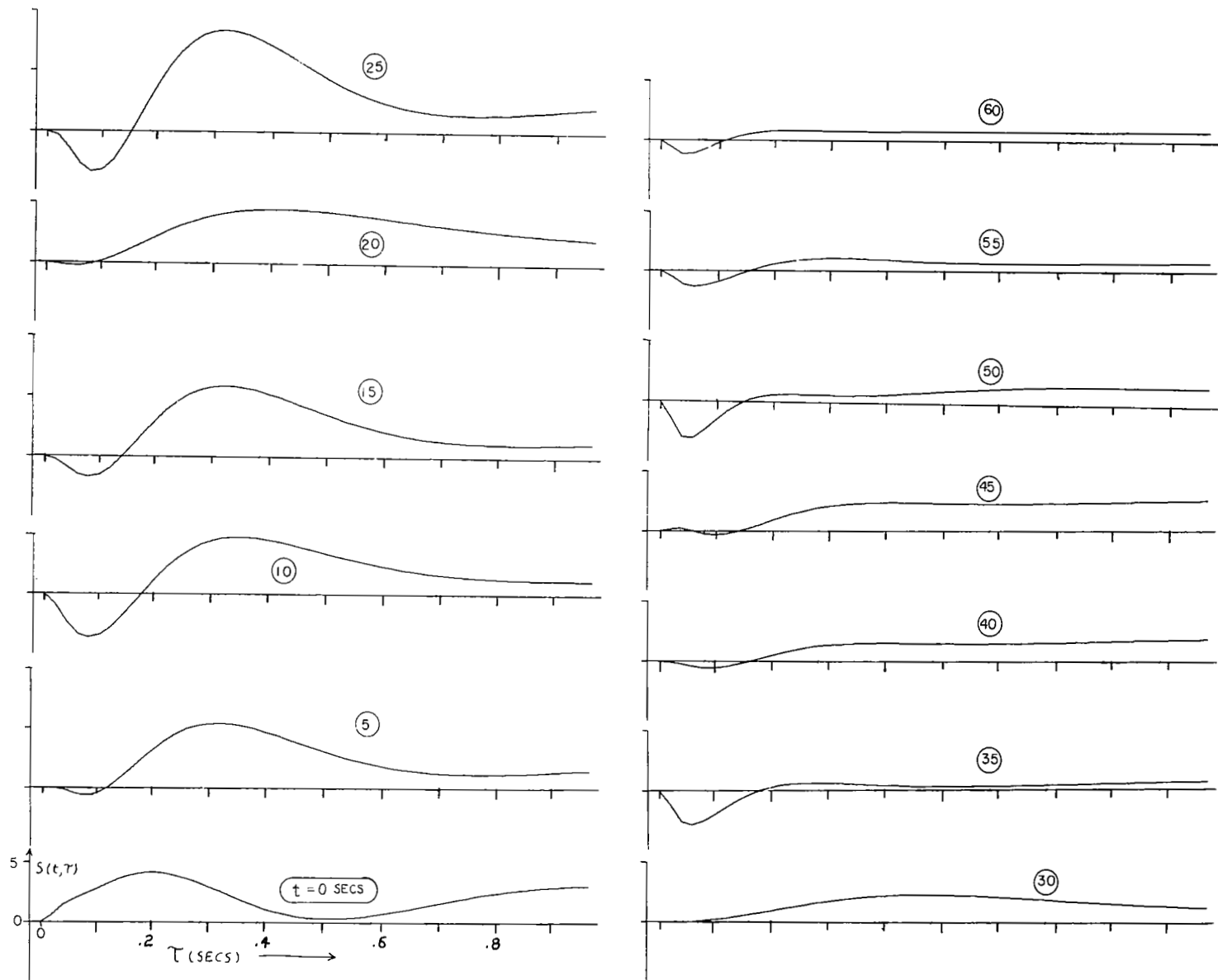


Figure 19 Plot of non-real-time special step response for Subject 1 characterization model (Experiment 3).

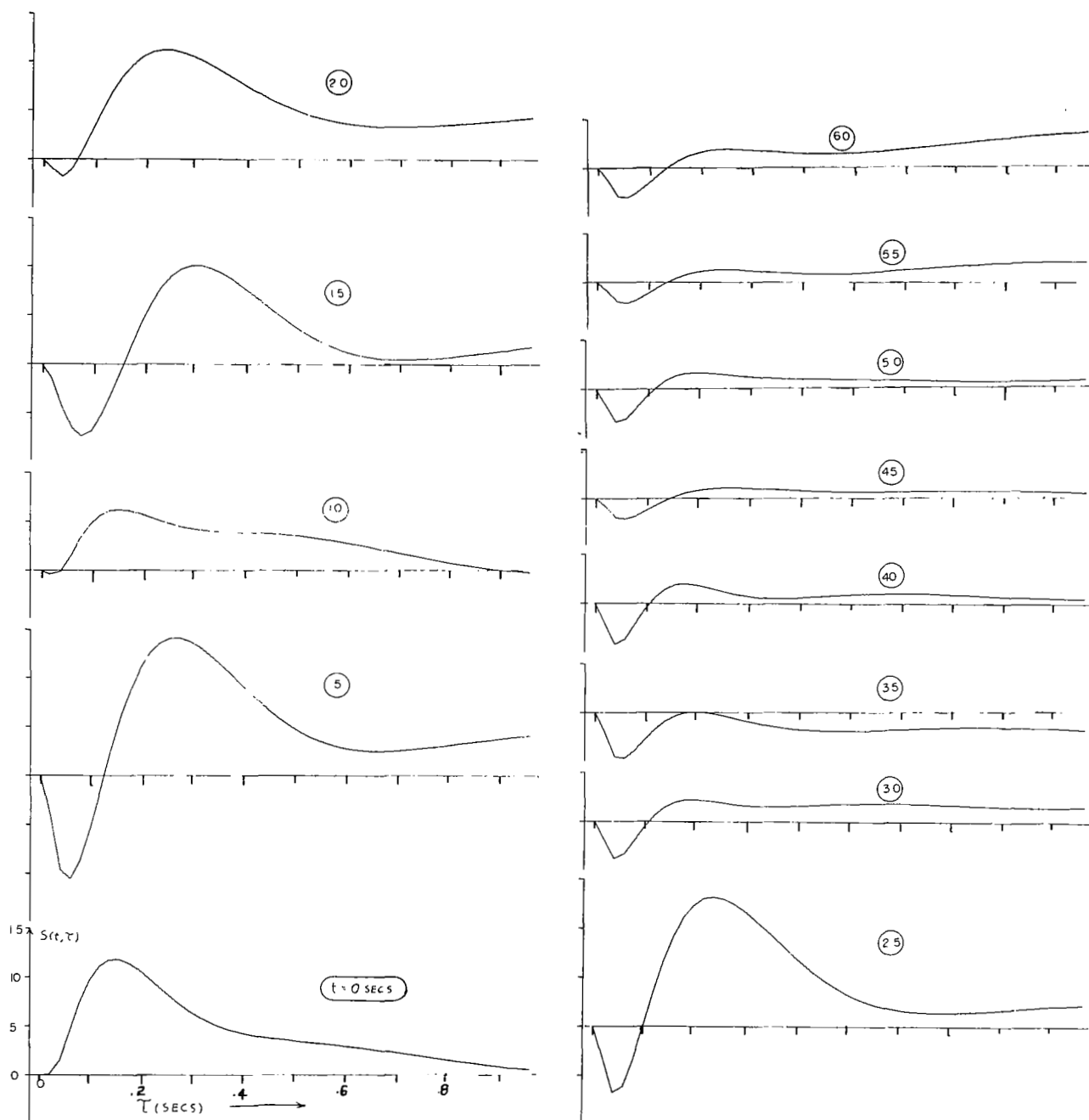


Figure 20 Plot of non-real-time special step response for Subject 2 characterization model (Experiment 3).

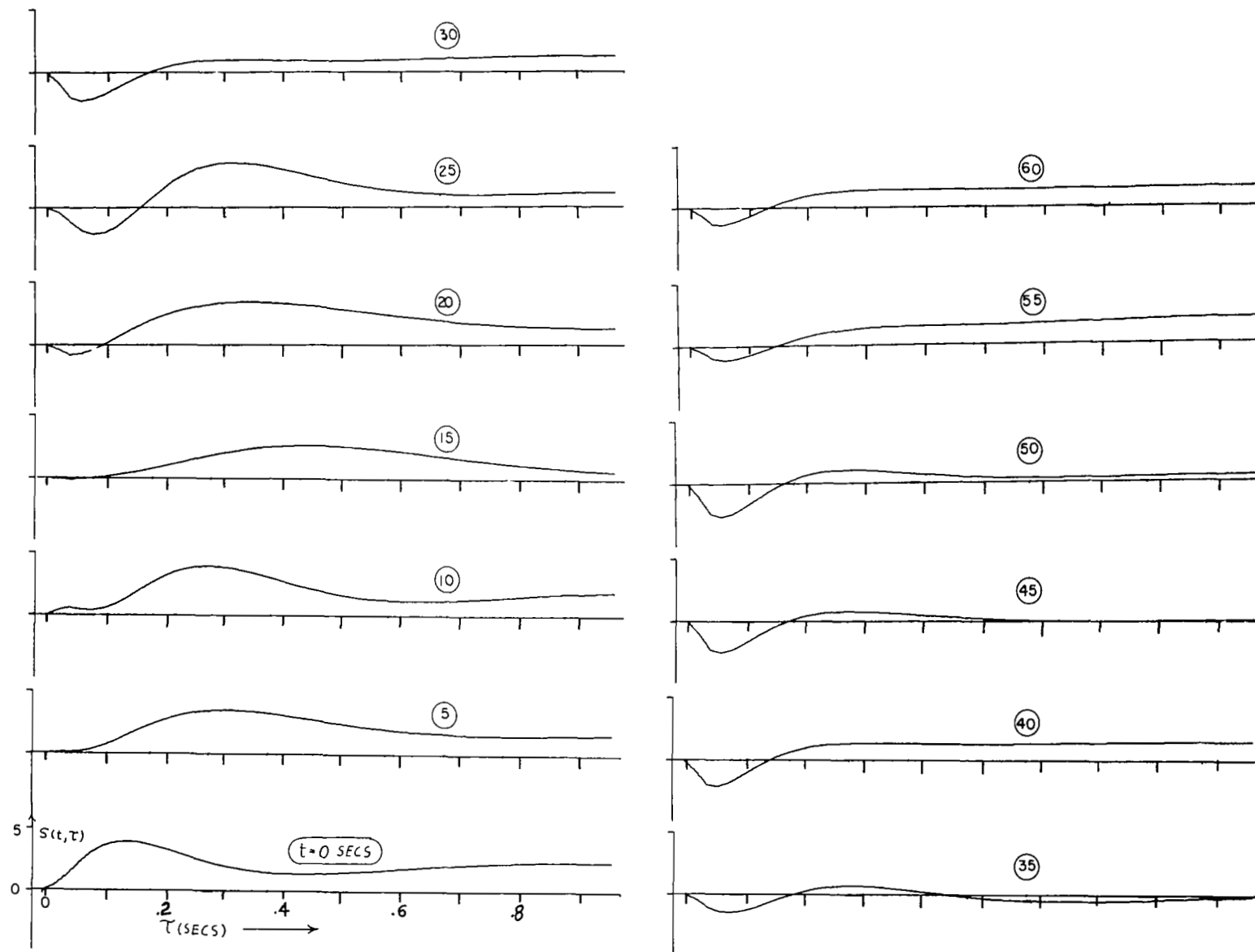


Figure 21 Plot of non-real-time special step response for Subject 3 characterization model (Experiment 3).

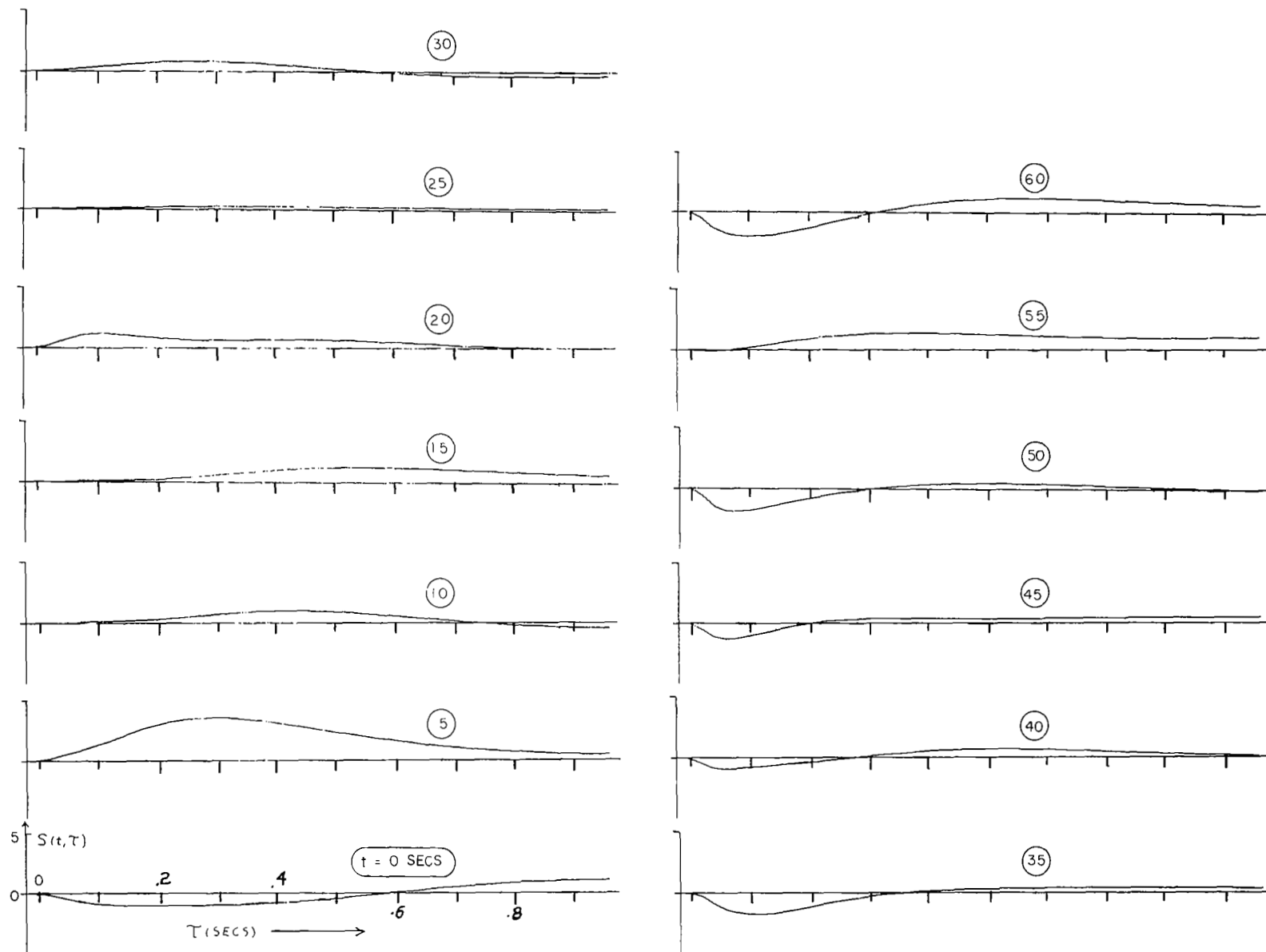


Figure 22 Plot of non-real-time special step response for Subject 4 characterization model (Experiment 3).



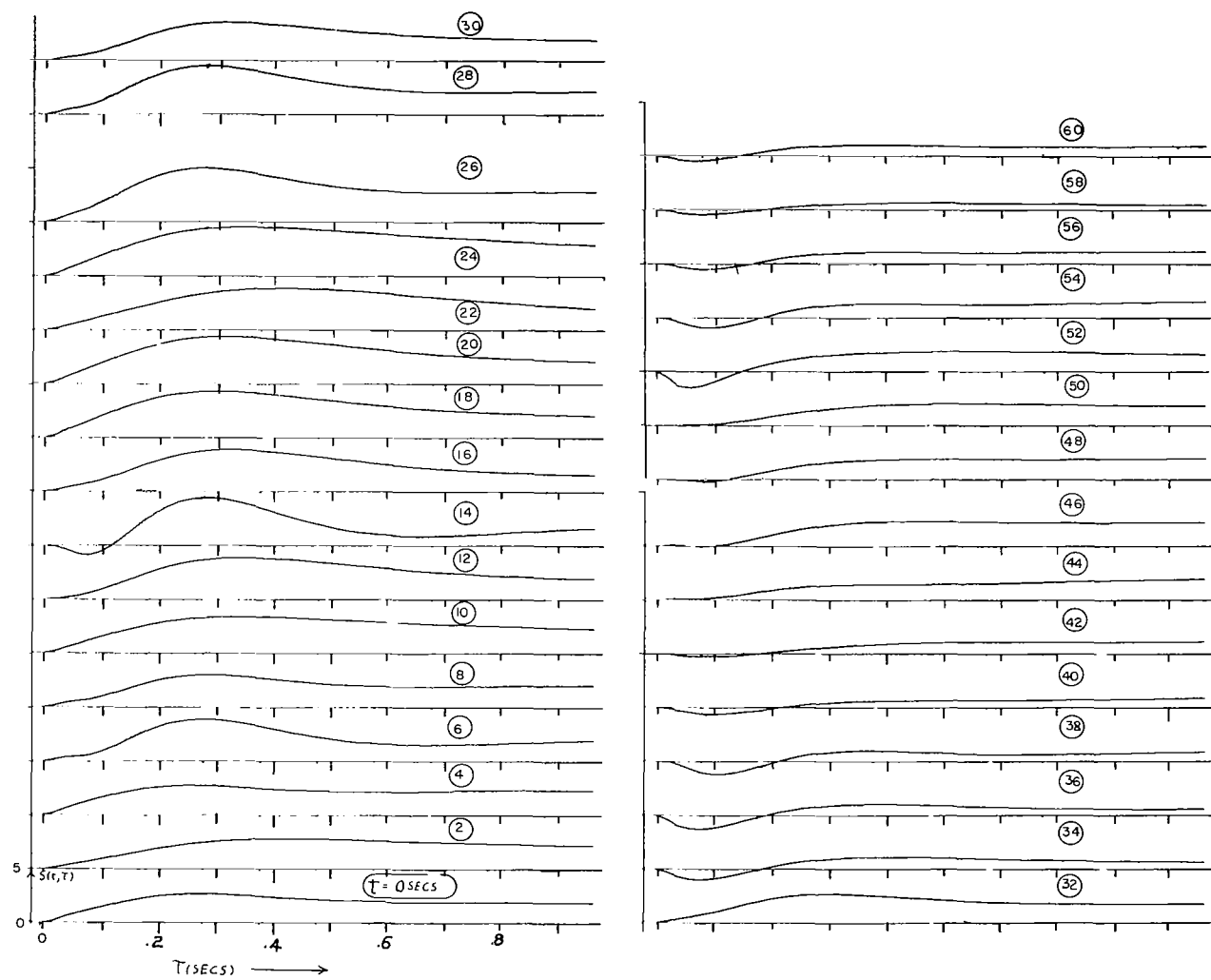


Figure 23 Plot of real-time special step response for Subject 1 characterization model (Experiment 3).

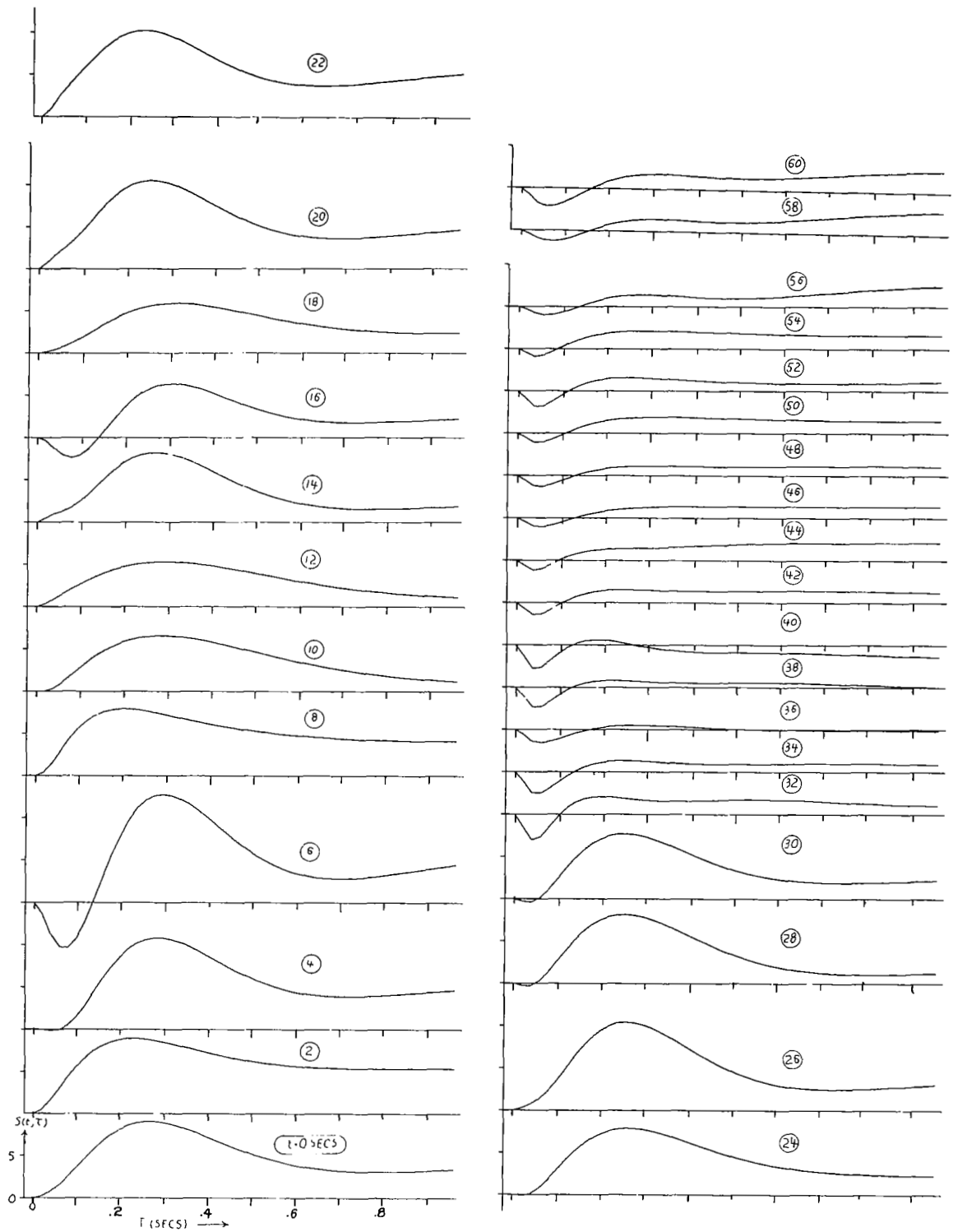


Figure 24 Plot of real-time special step response for Subject 2 characterization model (Experiment 3).

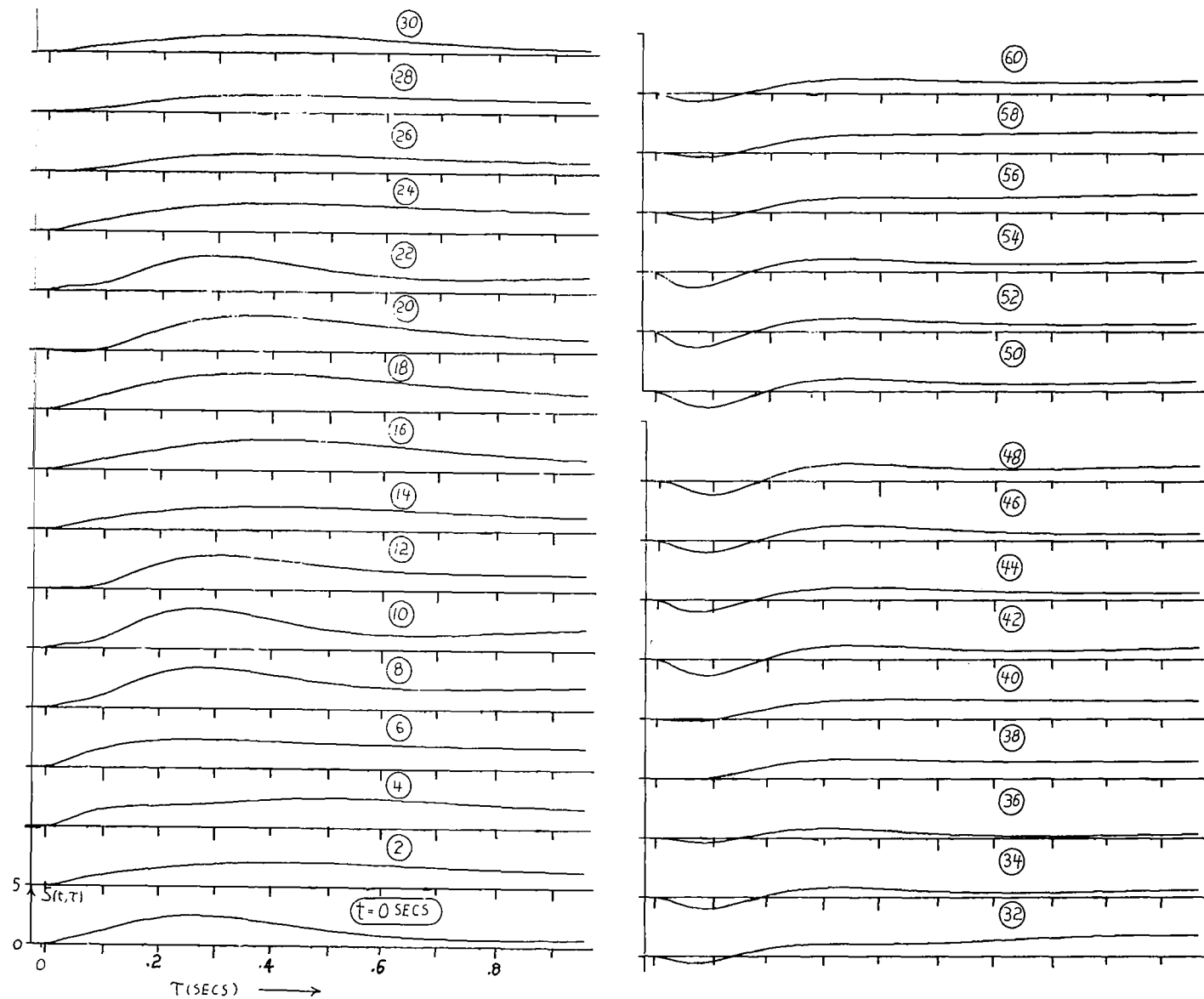


Figure 25

Plot of real-time special step response for Subject 3 characterization model (Experiment 3).

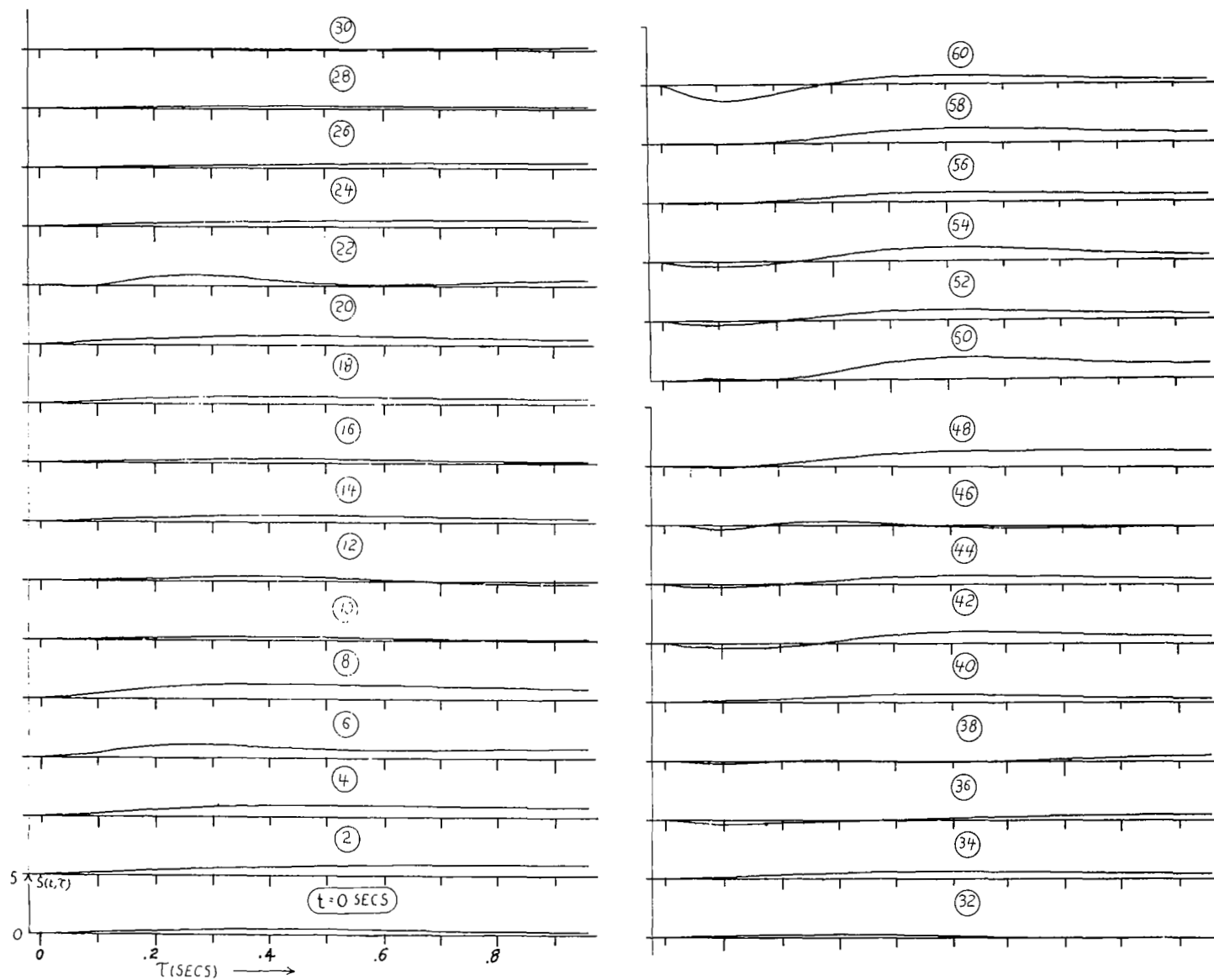


Figure 26

Plot of real-time special step response for Subject 4 characterization model (Experiment 3).